



**SCIENTIFIC COUNCIL MEETING – JUNE 2010**

Interdisciplinary oceanographic observations of Orphan Knoll

B. J. W. Greenan, I. Yashayaev, E. J. H. Head, W. G. Harrison, K. Azetsu-Scott, W. K. W. Li,  
J. W. Loder and Y. Geshelin

Department of Fisheries and Oceans, Maritimes Region  
Bedford Institute of Oceanography  
P.O. Box 1006, Dartmouth, N.S. B2Y 4A2

**Abstract**

An investigation of the oceanographic and lower trophic level biology has taken place in the region of Orphan Knoll, a NAFO closed area (NAFO/FC Doc. 06/5). This study has utilized existing data sets as well as collecting new data using shipboard and moored instrumentation. Physical properties indicate that mid-depth waters above Orphan Knoll are in a boundary region between outflow from the Labrador Sea (subpolar gyre) and northward flow of the North Atlantic Current (subtropical gyre). Near-bottom current measurements provide evidence for anti-cyclonic (clockwise) circulation around the knoll. A west-east gradient in nutrients was observed and is likely related to water mass differences between Orphan Basin and the region east of Orphan Knoll. The saturation state of seawater on the Orphan Knoll sediment surfaces is less than 1.2 and, therefore, organisms with shells and skeletons composed of aragonite and calcite with high magnesium content (more soluble than aragonite) may be affected by ocean acidification. The saturation state of seawater with respect to  $\text{CaCO}_3$  and the ecosystem response need to be monitored closely. Chlorophyll, small phytoplankton and bacteria in the Orphan Basin-Orphan Knoll region in the spring of 2008 and 2009 showed strong spatial and inter-annual variability, reflecting the complex physical dynamics and growth conditions in the region. Bacterial abundance appeared to be elevated on the summit of the knoll compared to surrounding waters at the same depth, but the persistence of this feature is not known. Zooplankton abundance was significantly greater in the region in 2009 relative to the preceding year, but no enhancement relative to the surrounding region was observed over Orphan Knoll. Overall, we have little evidence at this point that Orphan Knoll enhances the lower trophic level biology in the water column above the knoll; however, near-bottom anti-cyclonic circulation could have important implications for benthic community which will be surveyed in July 2010.

**1. Introduction**

Waters over the continental slope and rise off Atlantic Canada are in a highly advective regime because of their location in the western boundary (Labrador) current of the North Atlantic's subpolar gyre (Figure 1), and their close proximity to the energetic subtropical Gulf Stream System (GSS). Strong connectivity among the Atlantic Canadian shelf waters is clear, with major implications for how Atlantic Canadian shelf ecosystems will respond to climate change. However, the degree and nature of connectivity among the waters over the lower slope and rise is less clear in some cases, particularly in areas with complex topography, major frontal systems, and recirculations. There is additional complexity associated with the shelfward meandering of the North Atlantic Current (Gulf Stream extension) north of Flemish Cap and the projection of Flemish Cap and the Tail of the Grand Bank towards the GSS. As a result, there are competing influences of the major current systems favouring connectivity, and topographic obstructions such as seamounts favouring regional isolation or retention and biological endemism. There is very little historical oceanographic data collected on Orphan Knoll and, therefore, new data sets are providing an improved understanding of the degree to which the regional oceanography has the potential to establish conditions favouring the development of a unique marine environment (relative to the surrounding regions) on Orphan Knoll.

Five principal factors have been identified that determine the effects of isolated seamounts on the surrounding ocean (Lavelle and Mohn, 2010):

- the height of the seamount ( $h$ ) relative to the depth of the ocean ( $H$ )
- the vertical component of Earth's rotation rate ( $f/2$ ) determined by its latitude
- density stratification of the surrounding water
- the seamount length scale  $L$ , shape, flank slope ( $\alpha$ )
- and the energy-frequency distribution of the impinging steady and oscillating currents ( $U_{mean}$  and  $U_{var}$ ) and eddies.

NAFO closed areas (NAFO/FC Doc. 06/5) in the subtropical environment (e.g. Newfoundland Seamounts, New England Seamounts) contrast with those in the subpolar gyre (e.g. Orphan Knoll) in several ways including differences in the background flow, which are relatively weak in the subpolar gyre compared to that experienced by the seamounts in the subtropical gyre. Secondly, the lower temperature over the seamounts in subpolar waters will likely contribute to slower recovery of ecosystems in these areas. In addition, environmental factors such as increasing ocean acidification will have a higher impact in the colder regions such as those in the subpolar gyre.

About one third of the anthropogenic carbon dioxide ( $\text{CO}_2$ ) released since the start of the Industrial Revolution in the 1800s has been taken up by the oceans, altering the basic ocean chemistry, specifically the marine carbonate system. The dissolution of anthropogenic  $\text{CO}_2$  ( $\text{CO}_2$  released by human activities, mainly by fossil fuel combustion) has decreased ocean pH by 0.1 unit over the past 200 years. If global emissions of  $\text{CO}_2$  continue at their present rate, ocean pH is predicted to fall an additional 0.3 units by 2100. The oceans have not experienced such a rapid pH decrease (ocean acidification) or one of this great a magnitude for at least 650,000 years, raising serious concerns about the ability of marine ecosystems to adapt. The most direct impact will be to organisms that form calcium carbonate ( $\text{CaCO}_3$ ) shells and skeletons because acidity increases the solubility of  $\text{CaCO}_3$ . These organisms include phytoplankton such as coccolithophores, zooplankton such as pteropods and foraminifera, sea urchins, molluscs and corals. Since  $\text{CaCO}_3$  shells and skeletons are naturally more soluble in lower temperature and higher pressure, high latitude and deep water ecosystems will be more vulnerable to added stress of ocean acidification.  $\text{CaCO}_3$  comes with two forms, calcite and aragonite. Aragonite forming organisms are more at risk than calcite forming organisms because of higher solubility of aragonite. Some deep water corals have aragonite skeletons and live in cold, deep waters, so these organisms will be particularly vulnerable.

Oceanic seamounts are often referred to as “hotspots” of marine life due to the often observed enhancement of fish and rich benthic communities associated with these submarine features. Theory and observational research on the causes of this rich biological activity on seamounts has focused on localized perturbations of circulation fields and mixing. In principle, increased nutrient availability over seamounts enhance primary production which provides the energy to sustain production at higher trophic levels. However, despite local ephemeral enhancement of phytoplankton standing stocks, there have been few reports of persistent enhancement that is clearly identified as a direct effect of seamounts (Genin and Dower 2007). The initial reconnaissance of this study, therefore, was aimed at establishing if there is evidence of enhancement of nutrients over Orphan Knoll, relative to surrounding waters, and also if there is any indication of higher abundances of lower trophic levels (bacteria, phytoplankton, zooplankton) on the knoll.

The zooplankton community in the Newfoundland Shelf regions is dominated, in terms of biomass, by three large species of copepod, which all belong to the genus *Calanus*. *Calanus finmarchicus* is a boreal species, which is found throughout the North Atlantic north of the Gulf Stream, from the Gulf of Maine and Georges Bank in the southwest to the Barents Sea in the northeast. *Calanus glacialis* and *Calanus hyperboreus* are arctic species, which are found at more southerly latitudes where there are influxes of arctic water, notably in the Labrador and Newfoundland shelf and slope waters. *C. finmarchicus* has a one year life history, spending the winter at depth in a pre-adult stage, coming to surface to mature, mate, reproduce and develop in spring and summer. The arctic *Calanus* species have multi-year life cycles, spending two or more winters at depth as young stages and reproducing

in spring, or late winter, so that the youngest stages can feed during the phytoplankton growth season. Regional or inter-annual differences in abundances in spring/early summer generally reflect differences in the timing of reproduction and appearance of young stages and are generally linked to differences in water temperatures and spring bloom dynamics.

## 2. Methods

Ship-based observations of physical, chemical and lower-trophic level biology are the primary source of information utilized in this analysis. Annual surveys of the Orphan Knoll region were carried out three times in 2008-10 in the month of May. The 2009 survey was the most comprehensive of the three surveys. The 2008 and 2010 surveys were comprised mostly of physical and biological oceanography measurements with the primary purpose of these missions being to deploy and recover moorings.

Water samples were collected using a 24-bottle rosette attached to a CTD (SeaBird SBE 911). Nutrients (nitrate, silicate and phosphate) were analyzed colourimetrically using standard chemical methods and a Technicon Autoanalyzer and chlorophyll was determined on acetone-extracted samples by fluorometry (Mitchell et al. 2002). Nanophytoplankton, picophytoplankton and bacterial abundance was determined by flow cytometry according to methods outlined in Li and Dickie (2001).

Water samples were also analyzed for dissolved inorganic carbon (DIC) and total alkalinity (TA) on board within 24 hours of collection. 233 samples were analyzed for DIC and TA in 2008 and 401 samples for DIC, TA and pH in 2009. The carbonate system measurements, namely DIC, TA and pH, were conducted following the international protocol of Dickson *et al.* (2007). The DIC was determined using gas extraction and a coulometric method with photometric detection (Johnson, et al., 1985). The TA was measured by open-cell potentiometric titration with a five-point method (Haraldsson et al., 1997). The pH was measured by a spectrophotometric method (Dickson, et al., 2007). We report pH in total scale ( $\text{pH}_T$ ) at in situ temperature and pressure. Certified Reference Material (CRM) (supplied by Professor Andrew Dickson, Scripps Institution of Oceanography, San Diego, USA) was analyzed in duplicate every 20 samples to evaluate accuracy. Precision calculated from the differences of duplicate CRM measurements for DIC, TA and pH during the cruise were 0.05%, 0.09% and 0.002, respectively.

The saturation state of seawater with respect to  $\text{CaCO}_3$  (expressed in  $\Omega$ ) is a measure of its corrosiveness for the shells and skeletons of marine organisms. Without protective mechanisms, under-saturated seawater ( $\Omega < 1$ ) is corrosive to calcifying organisms. Furthermore, biological impairment can occur at saturation states with  $\Omega_{\text{arg}}$  as high as 3.1 for some organisms such as reef building corals (Kleypas *et al.*, 1999; Langdon and Atkinson, 2005).

Zooplankton samples were collected in the 0-100 m depth range by means of vertical ring net hauls using a 200  $\mu\text{m}$  mesh of 0.75 m diameter. Depth stratified vertical net hauls were carried out using a Hydro-bios Multi-net system, which had a square opening of 0.5 m x 0.5 m and which was fitted with five 200  $\mu\text{m}$  nets, which could be opened/closed at specified depths.

In addition to the shipboard measurements, moorings were deployed on Orphan Knoll for the period 2008-2010 (Figure 2). While the measurement parameters on the moorings were primarily limited to near-bottom currents, temperature, salinity and dissolved oxygen concentration, these instruments provide measures of variability which are not feasible from ship occupations once a year. Moorings with a Aanderaa RCM11 acoustic current meter (25 m above bottom) and SeaBird SBE37 Microcat conductivity/temperature/depth sensor (50 m above bottom) were deployed at sites OK-A (2200 m), OK-B (1750 m) and OK-C (2200 m) in May 2008 on cruise HUD2008006 (Figure 2) and recovered in May 2009 on cruise HUD2009011. The current meters provided samples once per hour and the Microcats recorded every 5 minutes. Moorings were deployed in May 2009 at sites OK-D (2200 m), OK-B (1750 m) and OK-E (2200 m). This set of moorings on the flanks of the knoll were designed similar to the moorings deployed in 2008-09, however, the OK-B mooring at the summit of the knoll included additional instrumentation for the 2009-10 deployment; this mooring included two Aanderaa RCM11 acoustic current meters with Optode dissolved oxygen sensors included at depth of 1300 m and 12 m above bottom (nominally 1738 m). SeaBird SBE37 Microcats deployed on the mooring at 1000 m and 1550 m. The OK-B mooring was recovered in May 2010 on cruise HUD2010009. It was decided that in order to provide measurements of currents during the period of HUD2010029, led by Dr. E. Kenchington, the moorings at OK-D and OK-E would be left in place until July 2010. In addition, another near-bottom mooring was deployed in May 2010 at OK-C with the substitution of an RDI

Workhorse 300 kHz acoustic Doppler current profiler. This will provide a measure of the structure of currents over a range of approximately 100 m. In May 2010, communication with the acoustic release at OK-E was initiated and positioning of the mooring was confirmed. However, communication was not established with the mooring at OK-D during HUD2010009 and it is likely that the acoustic release has failed on this mooring. There were problems noted with this mooring during the deployment process and recovery is unlikely. In July 2010, mooring recoveries will be carried out at OK-C, OK-E and attempted once again at OK-D.

This project is also utilizing data collected through the Argo Programme, an international project which is a major component of the oceans observing system. Approximately 3000 profiling floats are deployed around the world. These floats sink to a target depth of 2000 meters for a preprogrammed period of time and then ascend to the surface, taking temperature and salinity values during the ascent. At the surface, the float drifts along for a day or two and transmits the data to a satellite run by Service Argos which then determines the position of the float. Service Argos sends the data to various data centers such as the DFO Integrated Science Data Management (ISDM) office. Floats which drift into the Orphan Knoll region will be used to provide spatial analysis of temperature and salinity.

Satellite remote sensing provide large-scale context for sea surface temperature (SST) and surface chlorophyll concentrations in the Orphan Basin-Orphan Knoll region during the period of field surveys in 2008 – 2010. Data were extracted from semi-monthly AVHRR SST and MODIS ocean color satellite imagery: (<http://www.mar.dfo-mpo.gc.ca/science/ocean/ias/remotesensing.html>).

The Ocean Features Analysis (OFA) chart is a combination of SST and added boundary lines for water masses and eddies which is produced by the Department of National Defence Canada METOC office. AVHRR composites for the previous 3 days (or since the previous OFA) are blended with surface temperatures from ships, ARGO data, XBT reports from ships, and buoy data (and sometimes AZMP data). Ship and buoy reports are downloaded from ISDM. METOC carries out quality control on all data and removes outliers. The Ocean WorkStation (OWS) software then uses a kriging technique to blend all the observations together, along with monthly historical climatology (provided by Igor Yashayaev, BIO) to produce a temperature field. Guidance from US Navy models and other SST composite images is used (especially in winter) when satellite coverage is sparse. Once the SST field is derived, the water mass boundary lines are added manually, using guidance based on monthly temperature characteristics.

### 3. Results

#### 3.1 Physical Oceanography

##### 3.1.1 CTD Survey

A cross-section of potential temperature in Orphan Basin and Orphan Knoll provides some insight into interannual variability in this region (Figure 3). At the depth of the summit on Orphan Knoll, the temperature in 2009 was approximately 0.3°C warmer than the preceding year. In the upper 500 m of the water column, the change was approximately 1-3°C warmer in 2009. However, horizontal variability in this upper layer is significant and the warm water mass appears to be limited to the region of Orphan Knoll and approximately 100 km to the west. Doming of the isotherms is observed in 2008 for several hundred meters above the knoll summit. Doming isotherms in western Orphan Basin in 2009 (at ~180 km) indicate the occurrence of a mesoscale eddy, a feature which has been observed on previous transects of the basin.

Denmark Strait Overflow Water (DSOW) is observed near bottom on both the east and west sides of Orphan Knoll. North East Atlantic Deep Water (NEADW) is present in the depth range of 2000-2500 m in this region; the extent of this water mass is more evident in the salinity field for this region (Figure 4). Labrador Sea Water (LSW), which is formed by vertical overturning during the winter, is clearly observed in the 2008 transect of Orphan Basin (Figure 3). The depth of convection in the Labrador Sea is primarily determined by surface heat fluxes in the west central Labrador Sea, changes in the warm and saline inflows in the West Greenland Current, and changes in Arctic fresh water inputs. The cooling and densification of the upper levels of the west-central Labrador Sea observed in the 2008 winter interrupted a recent warming trend at intermediate depth levels, however, the milder air temperatures during the winter of 2009 limited convection and the warming trend has resumed in 1000-1500 m layer.

### 3.1.1 Remote Sensing (SST)

Analysis of sea surface temperature features is provided by METOC for the periods coinciding with the field expeditions in 2008 and 2009 (Figure 5) as well as from the BIO Ocean Monitoring and Research Section (ORMS, Figure 6). The SST in the Orphan Knoll region is consistent with near-surface data collected with the shipboard CTD. It is apparent from the SST analysis that temperature in the region was warmer in 2009 due to the incursion of a filament from a meander of the North Atlantic Current (NAC) in the subtropical gyre. This underscores the fact that Orphan Knoll is influenced both by subpolar waters exiting the Labrador Sea as well as periodic episodes of subtropical waters from NAC meanders.

### 3.1.2 Moored Current Measurements

As stated above, unlike seamounts in the Northwest Atlantic subtropical gyre which experience strong background flows, Orphan Knoll exists in a region with relatively weaker flow. Measurement of current rate 25 m above bottom (mab) at each of the mooring sites for the period May 2008 – May 2009 (Figure 7) indicate that flow on the east flank of the knoll is stronger and more variable (OK-C, mean  $0.085 \text{ m s}^{-1}$ , std.  $0.047 \text{ m s}^{-1}$ , max  $0.32 \text{ m s}^{-1}$ ) than encountered on the west flank (OK-A, mean  $0.041 \text{ m s}^{-1}$ , std.  $0.025 \text{ m s}^{-1}$ , max  $0.20 \text{ m s}^{-1}$ ) or at the summit (OK-B, mean  $0.043 \text{ m s}^{-1}$ , std.  $0.023 \text{ m s}^{-1}$ , max  $0.15 \text{ m s}^{-1}$ ).

A spectral analysis of the near-bottom currents (Figure 8) indicates that the M2 (semi-diurnal) tide contributes to the variability at all three mooring sites with the spectral peak being most dominant on the east flank. Spectral energy is also evident at harmonics of the M2 tide. The K1 (diurnal) tide does not appear to be an important factor in these near-bottom currents.

A progressive vector diagram (Figure 9) demonstrates the flow on the west flank of Orphan Knoll (OK-A) is fairly consistently in the northwest direction travelling approximately 400 km over the period of one year. The flow on the summit (OK-B) is predominantly to the south, however, the direction is more variable than that observed on the west flank and the distance traversed in the period of one year is about 200 km. On the east flank (OK-C), there are two periods of quite consistent flow to the southeast interspersed with other periods in which the flow is more variable and predominantly to the southwest. This PVD suggests that there exists an anti-cyclonic (clockwise) flow around the knoll. This is consistent with theory for such topography in the Northern Hemisphere. This flow could either be due to: 1) the formation of a Taylor cap over the knoll which is a result of topographic blocking of the background flow, or 2) the process of tidal rectification which results in a residual flow due to tidal forcing.

The near-bottom currents on Orphan Knoll are presented in context of the region in Figure 10. The annual mean flow at all mooring sites follows topography with current in the western part of Orphan Basin being substantially larger than observed in the eastern part of the basin and on Orphan Knoll. Interannual variability is small for sites at which multi-year data sets exist.

### 3.1.3 Argo Floats

An analysis of drift of Argo floats between successive profiles (Figure 11) infers that currents over the summit of Orphan Knoll are very weak. These profiling floats drift for approximately 9 days at a depth of 1500 m and, subsequently, descend to 2000 m prior to ascending to the surface. Temperature and salinity is measured with an onboard CTD during the ascent and then transmitted via satellite while the profiler is at the ocean surface. It should be noted that there is the possibility that Argo floats over the top of the knoll would hit the bottom and this could have some impact on the drift results. However, the time a profiler would spend on bottom would likely be only a small percentage of the total drift time. We plan to also utilize drifters from previous research programs, such as the World Ocean Circulation Experiment, to attempt to improve our estimate of circulation above the knoll.

Argo floats have been used to develop a climatology at mid-depth (650-950 m) for temperature and salinity in the Orphan Basin/Orphan Knoll region (Figure 12). These results indicate that Orphan Knoll appears to be located in a boundary region between outflow from the Labrador Sea (observed in Orphan Basin) and the northward extension of the North Atlantic Current. This could have implications for the connectivity between Orphan Knoll and the

surrounding environment since nearby topographic features such as Flemish Cap are predominantly influenced by outflow from the subpolar gyre in this depth range.

### 3.2 Chemical Oceanography

#### 3.2.1 Nutrients

Nutrient sections from the 2009 survey showed some structure in nutrient concentrations, particularly in the upper 500 m, that indicated some degree of “doming” (shallowing) of concentrations along the margins and on the summit of Orphan Knoll (Figure 13). However, in near surface waters (<100m) concentrations were near detection limits and no enhancement of concentrations at the edges or on top of the Knoll was evident. All nutrient fields also have west-east gradients, which is likely linked to the differences in water masses observed in the Argo T/S climatology for the region.

#### 3.2.2 Ocean Acidification

Low pH was observed at the deep waters of southern and eastern sides of Orphan Knoll (Figure 14). In the surface 2000m, an east-west gradient of pH distribution is relatively small (OBB line), while the north-south gradient is stronger. Lower pH is observed on the Orphan Knoll compared to the Orphan Basin and toward the shelf. Saturation states for calcite ( $\Omega_{\text{cal}}$ ) and aragonite ( $\Omega_{\text{arg}}$ ) are shown in Figure 15 and Figure 16. The saturation horizon for aragonite ( $\Omega_{\text{arg}}=1$ ) is around 2000-2500m and shoaled from the south and east towards the Orphan Knoll.  $\Omega_{\text{cal}}$  is higher than 0 through out the sections. Since the saturation state of seawater on the sediment surfaces are less than 1.2, organisms with shells and skeletons composed of aragonite and calcite with high magnesium content (more soluble than aragonite) may be affected by ocean acidification. The saturation state of seawater with respect to  $\text{CaCO}_3$  and the ecosystem response need to be monitored closely.

### 3.3 Biological Oceanography

#### 3.3.1 Zooplankton

*Calanus finmarchicus* in the near surface layer (0-100m) was relatively evenly distributed in both 2008 and 2009, although it was more abundant in 2009 (Figure 17). This was because young stages were more abundant, *i.e.* reproduction had started earlier. As well, in 2009 the young stage population was more developed on the Knoll than farther inshore, indicating that reproduction started earlier there. The two arctic *Calanus* species were most abundant at stations most influenced by arctic water, *i.e.* the Newfoundland slope waters, and again they were more abundant in 2009 than in 2008 because of a higher number of young stages. The differences are probably related to differences in temperature and the dynamics of the spring bloom.

Three small copepod species were very abundant in the Orphan Basin/Orphan Knoll regions. The Atlantic species, *Oithona atlantica*, and the arctic genus, *Microcalanus*, were both more abundant in 2008 than in 2009 (Figure 18). The former mainly occurred at offshore stations and around the Knoll, whereas the latter were most abundant in the slope waters near the shelf-edge. Whether these differences reflect differences in the influx of Atlantic or arctic waters, or in productivity is not clear. The abundance of the ubiquitous species, *Oithona similis*, was relatively even over all stations and between years.

In 2009 depth stratified tows were carried out at four stations: one in Orphan Basin, two on the flanks of the Knoll and one on top of the Knoll (Figure 19). Zooplankton biomass was concentrated in the 0-100 m layer at all stations, and species composition varied with depth and among stations. There was no evidence of increased zooplankton biomass associated with Orphan Knoll, either in the near-surface layers or at depth.

### 3.3.2 Phytoplankton (including remote sensing of chl)

Highest vertically-integrated (0-100 m) chlorophyll concentrations in 2008 and 2009 were observed on the SW boundary of Orphan Basin and at the margins of Orphan Knoll; lowest concentrations were seen on the top of the Knoll (Figure 20). Overall, concentrations were similar between the two survey years. The high chlorophyll concentrations observed at the boundary of the Orphan Basin were clearly evident in ocean colour imagery for 2008 and particularly 2009.

The abundance of nano-phytoplankton showed a similar distributional pattern to chlorophyll (Figure 21), however, concentrations were generally lower in 2009 than seen in the 2008 survey; concentrations generally increased west to east. Similarly, pico-phytoplankton abundance was highest along the margins of the Knoll and concentrations increased west to east (Figure 22). The longitudinal gradient of increasing cell abundance reflects the change from Arctic-influenced waters to Atlantic-influenced waters. In 2009 pico-phytoplankton abundance was lower, by ~50%, than observed in 2008.

### 3.3.3 Bacteria

The pattern of bacterial abundance showed highest integrated concentrations on and in proximity to Orphan Knoll in 2008 and 2009. Concentrations generally increased west to east, as seen in small phytoplankton, and integrated abundance was lower (~30%) in 2009 than seen in 2008 (Figure 23). In the 2008 hydrographic section, a local downward displacement of the isopleths of abundance is apparent at depths greater than 1500m in the waters immediately overlying the seamount (Figure 24), suggestive of downwelling in the core of a Taylor column. As a result, bacterial concentration on the seamount summit was elevated over that in surrounding waters at the same depth.

### Summary

The Orphan Basin-Orphan Knoll region is biologically rich and complex, and strongly influenced by local processes and advection. In the spring, the lower trophic level dynamics are likely dominated by the seasonal large-scale spring bloom event which would certainly mask any 'knoll-effect'. Investigations in other periods of the year could provide further insight into the role of this topographic feature in the lower trophic level dynamics.

Overall, we have little evidence at this point that Orphan Knoll enhances the lower trophic level biology in the water column above the knoll; however, near-bottom anti-cyclonic circulation could have implications for benthic community which will be surveyed in July 2010.

### Acknowledgements

Many staff and associates at BIO have contributed to this program which is funded by the DFO International Governance Strategy (IGS). In particular, the authors would like to thank Dr. Ellen Kenchington and Dr. Alain Vezina. The field expeditions are supported by skilled and dedicated staff in the Technical Operations Section of the Ocean Sciences Division and the Ocean Monitoring and Research Section in the Ecosystem Research Division. These efforts, together with those of the officers and crew of CCGS Hudson, are gratefully acknowledged.

### References

- Dickson, A.G., C. L. Sabine, and J. R. Christian (editors), 2007. Guide to Best Practices for Ocean CO<sub>2</sub> Measurements. *PICES Special Publication 3*, 191 pp.
- Genin A and J.F.Dower, 2007. Seamount plankton dynamics. In: Pitcher TJ, Morato T, Hart PJB, Clark MR, Haggan N, Santos RS (eds) *Seamounts: ecology, fisheries and conservation*. Blackwell, Oxford, pp 85-100.
- Haraldsson, C., Anderson, L.G., Hassellöv, M., Hulth, S., Olsson, K., 1997. Rapid high- precision potentiometric titration of alkalinity in ocean and sediment pore waters. *Deep-Sea Research*, I, 44, 2031-2044.

- Johnson, K.M., A.E. King and M.McN Sieburth, 1985. Coulometric TCO<sub>2</sub> analyses for marine studies: An introduction. *Marine Chemistry*, 16, 61-82.
- Kleypas, J.A., R.W. Buddemeier, D. Archer, J.-P. Gattuso, C. Langdon, B.N. Opdyke, 1999. Geochemical consequences of increased atmospheric carbon dioxide on coral reefs. *Science*, 284, 118-120.
- Langdon C. and M.J. Atkinson, 2005. Effect of elevated pCO<sub>2</sub> on photosynthesis and calcification of corals and interactions with seasonal change in temperature/irradiance and nutrient enrichment. *J Geophys Res* 110: C09S07. doi:10.1029/2004JC002576.
- Lavelle, W. and C. Mohn, 2010. Motion, commotion, and biophysical connections at deep ocean seamounts. *Oceanography*, 23, 90-103.
- Li W.K.W. and P.M. Dickie, 2001. Monitoring phytoplankton, bacterioplankton, and virioplankton in a coastal inlet (Bedford Basin) by flow cytometry. *Cytometry* 44:236-246.
- Mitchell M.R., W.G. Harrison, K. Pauley, A. Gagne, G. Maillet and P. Strain (editors), 2002. Atlantic Zonal Monitoring Program: Sampling Protocol. *Can. Tech. Rep. Hydrogr. Ocean Sci.* 223, 23 pp.

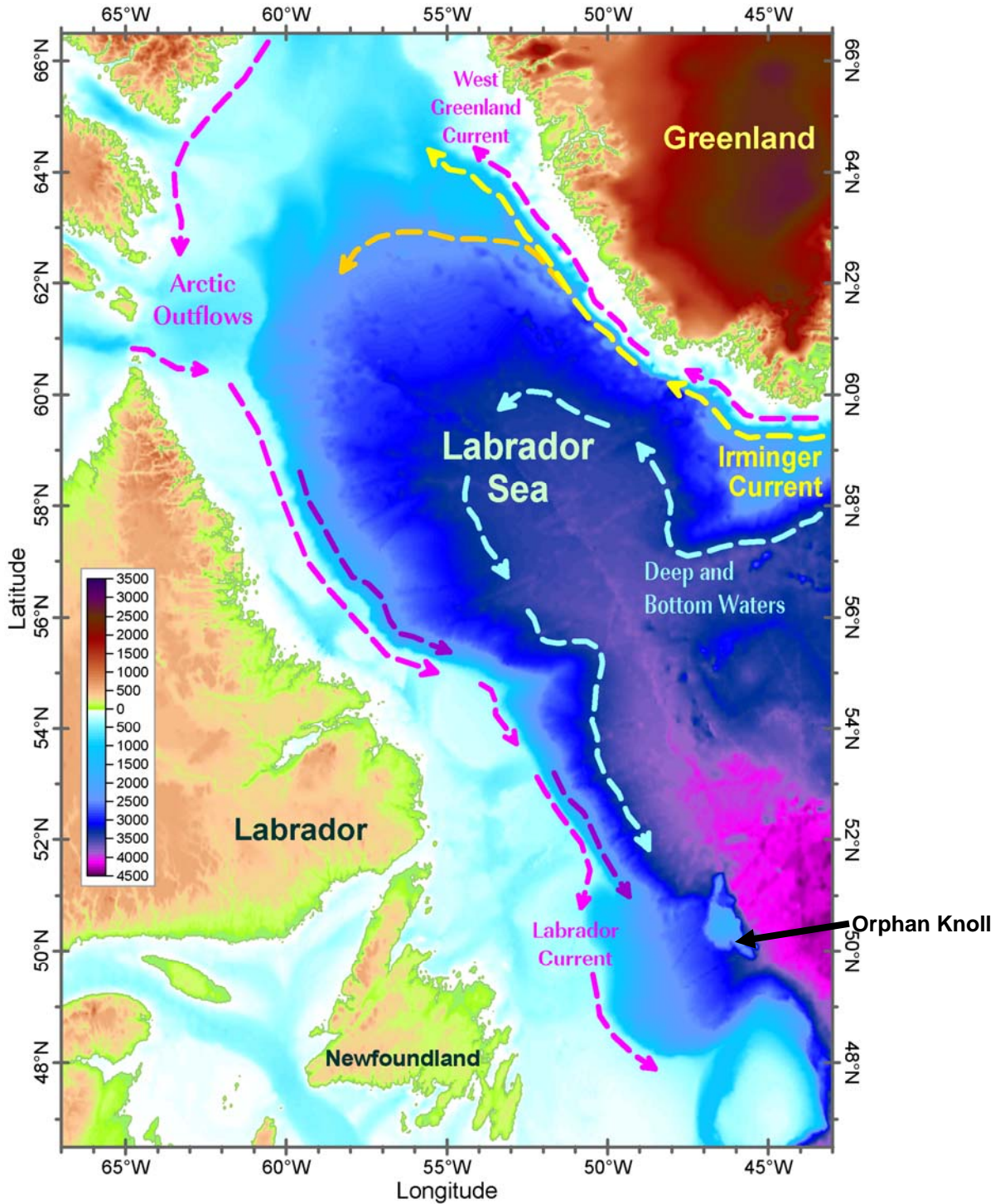


**Figure 1:** Circulation in the Labrador Sea region consists of upper layer currents along the edge of the Greenland and Labrador continental shelves (magenta lines). Deep and bottom waters (cyan line) enter this region south of Greenland and some of this water encounters Orphan Knoll as it exits the Labrador Sea.

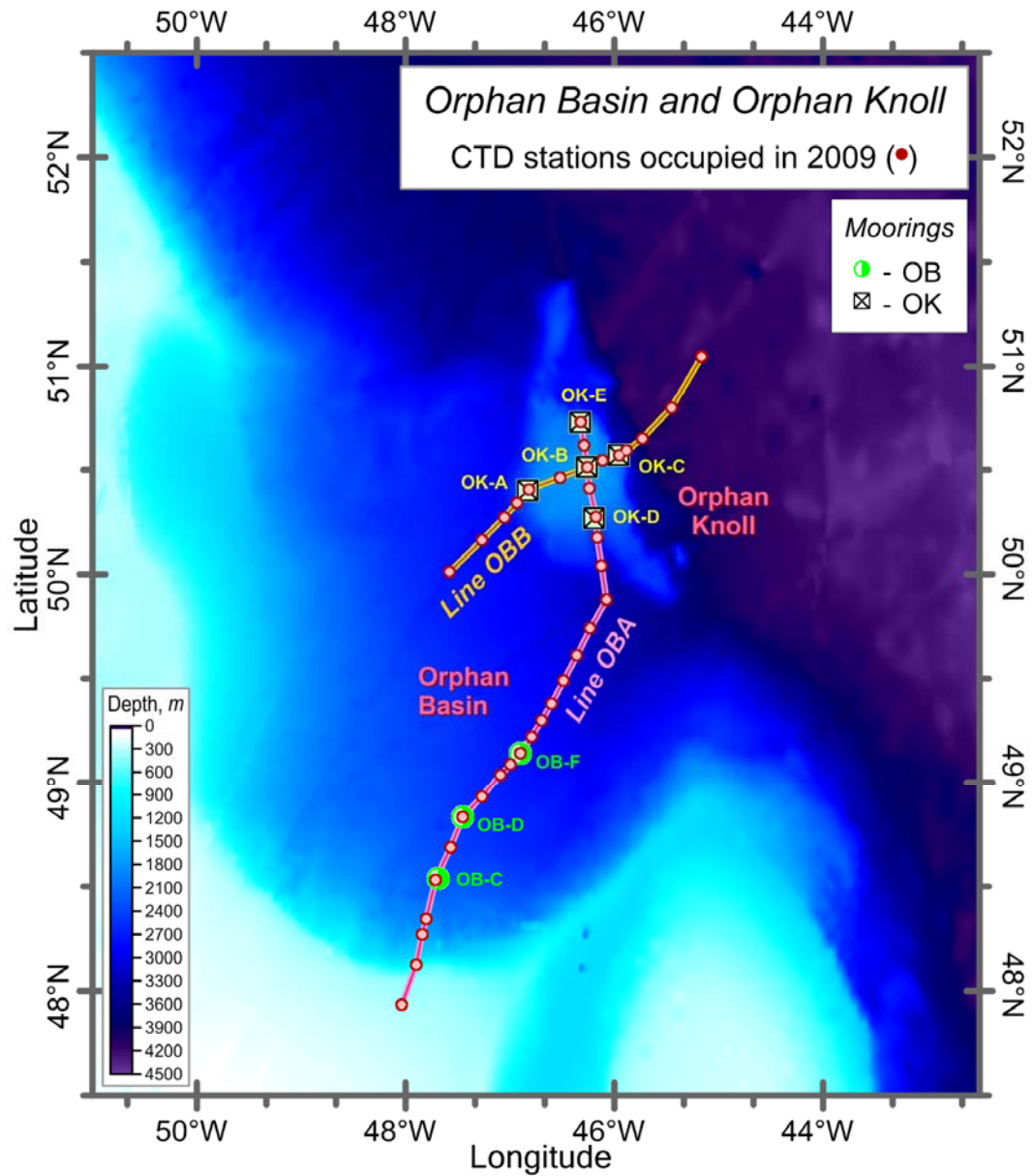


**Figure 2: Location of CTD stations (red circles) occupied in May 2009 during a cruise which combined Panel on Energy Research and Development (PERD)-funded research in Orphan Basin with DFO International Governance Strategy (IGS)-funded research on Orphan Knoll. PERD (green circles) and IGS (squares) moorings were deployed to provide year-round measurements of currents, temperature, conductivity and oxygen.**

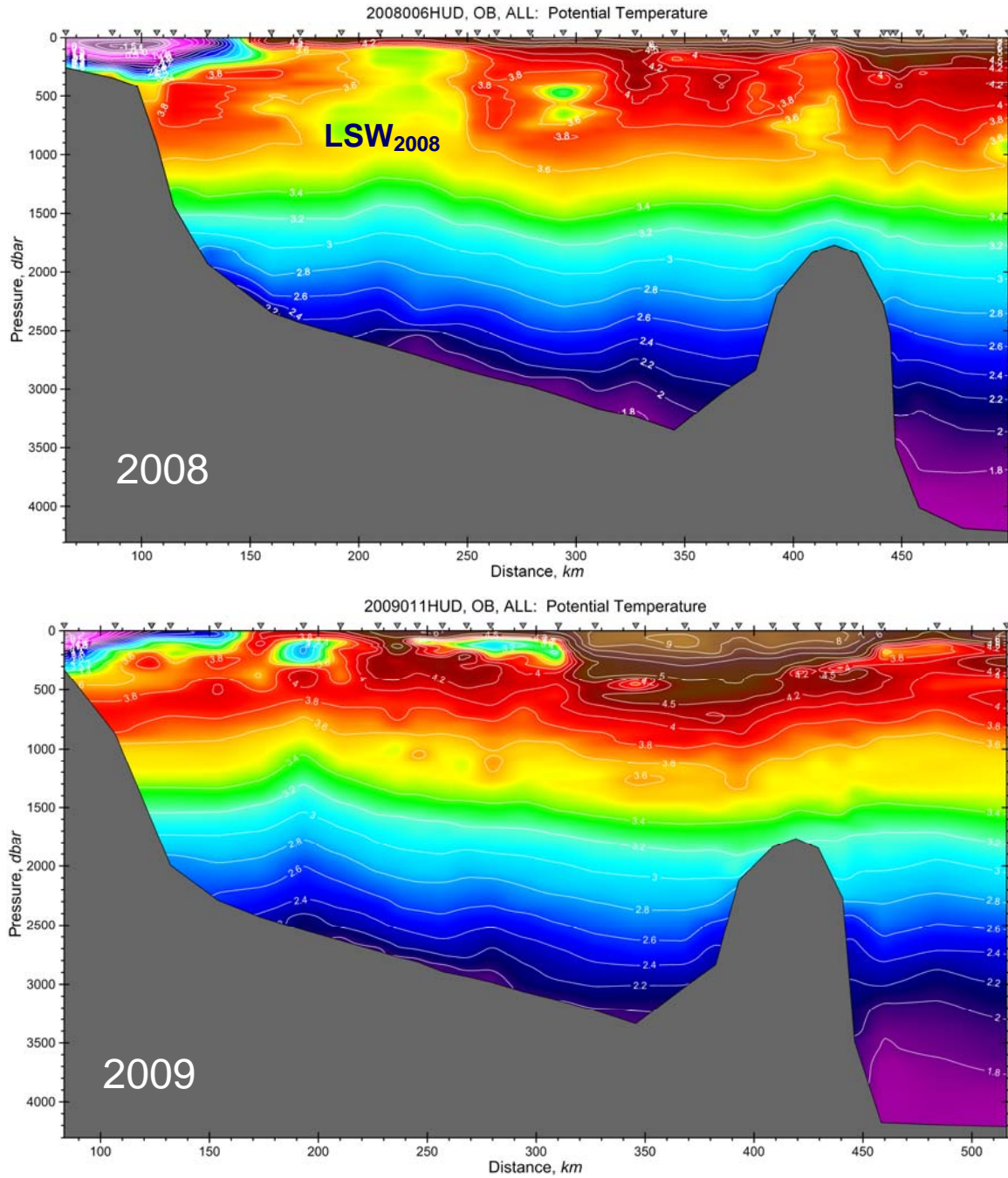


Figure 3: Potential temperature cross-section of Orphan Basin (0-350 km) and Orphan Knoll for 2008 and 2009 for Line OBA (see Figure 2).

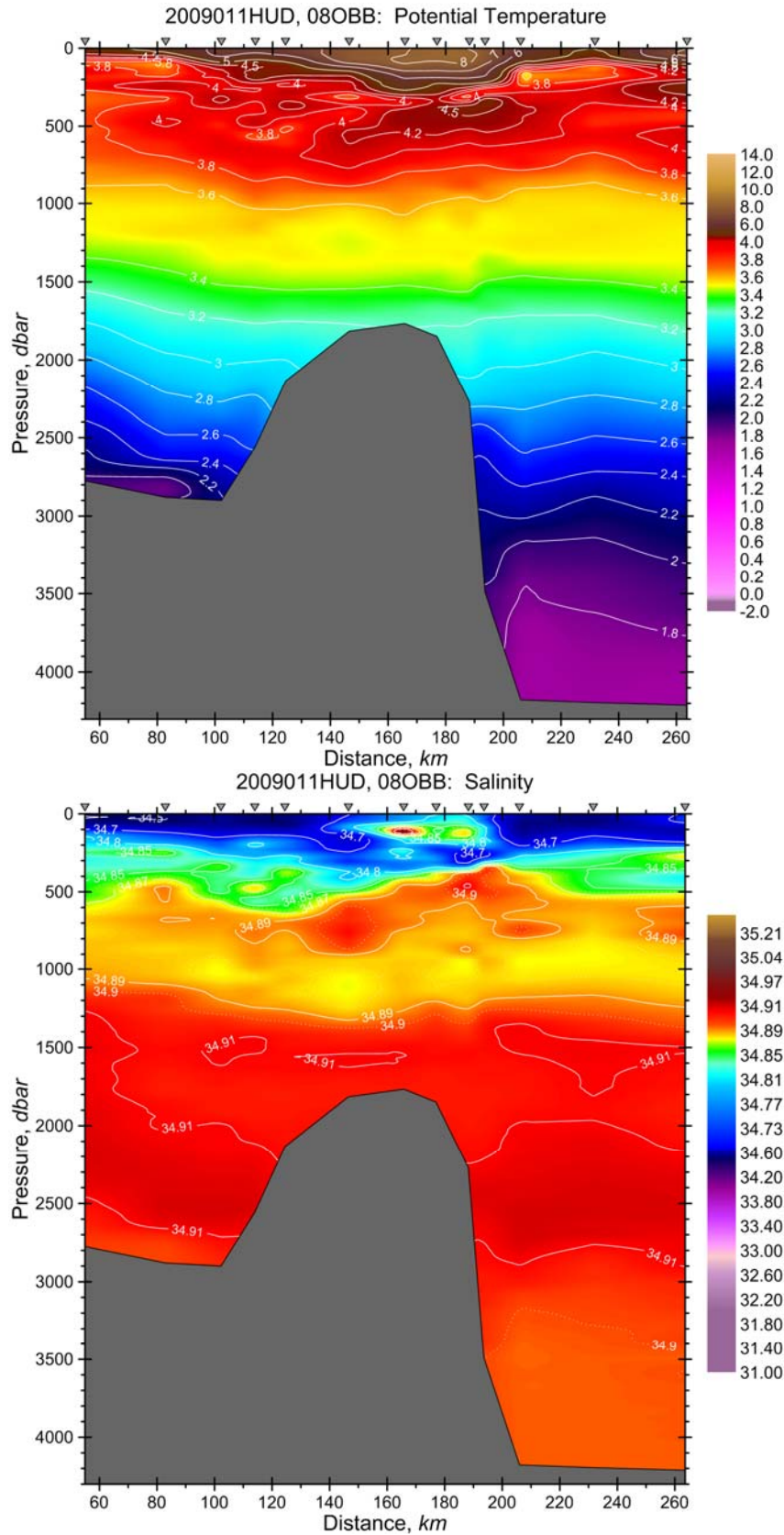


Figure 4: Potential temperature and salinity from the 2009 CTD survey of Orphan Knoll for Line OBB (see Figure 2).

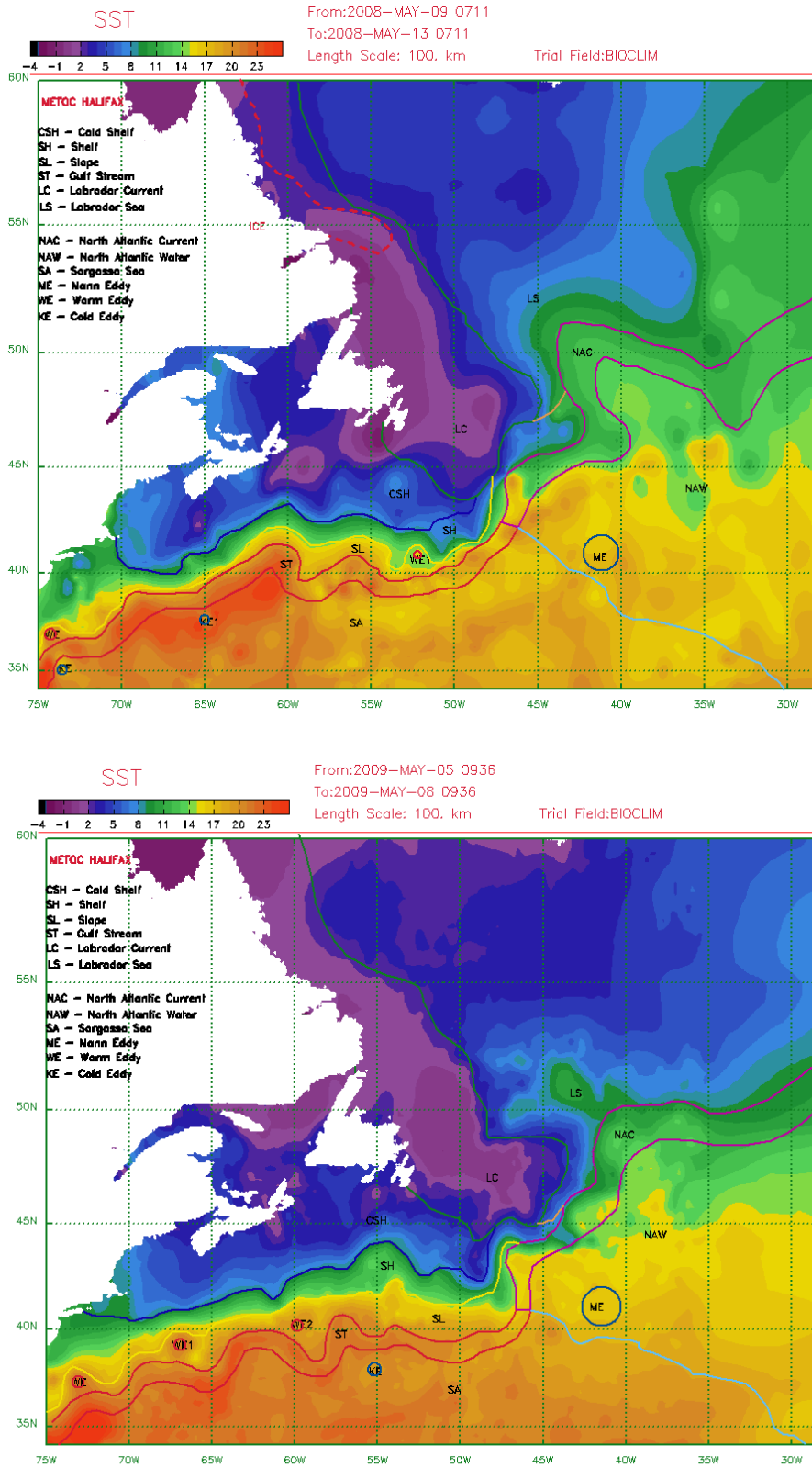


Figure 5: Sea surface temperature analysis for May 2008 and 2009 provided by METOC Halifax.

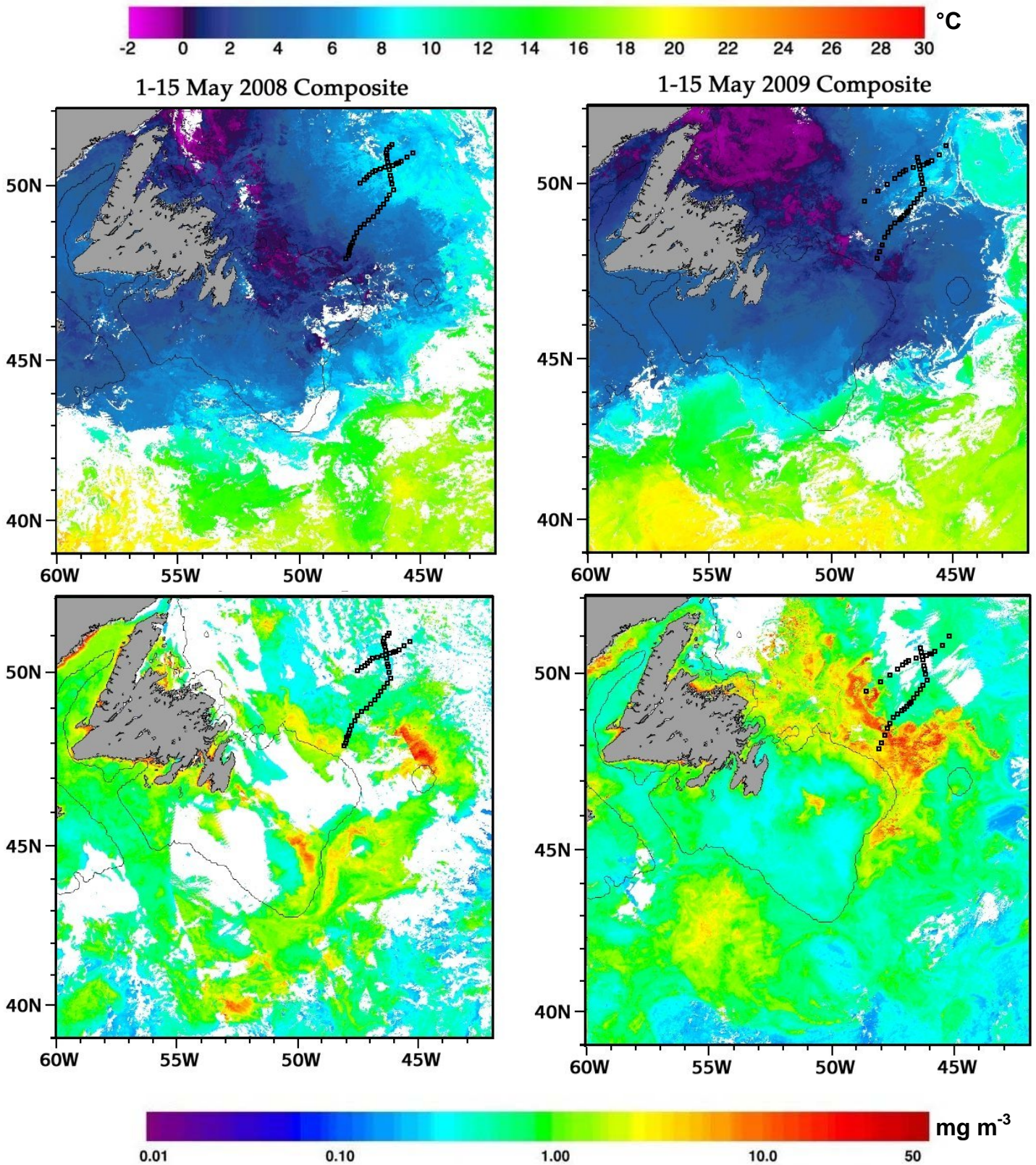


Figure 6: MODIS satellite sea surface temperature (top row) and chlorophyll concentration (bottom row) for the first half of May in 2008 (left column) and 2009 (right column). Locations of CTD stations in each of the field expeditions is indicated by the open squares.

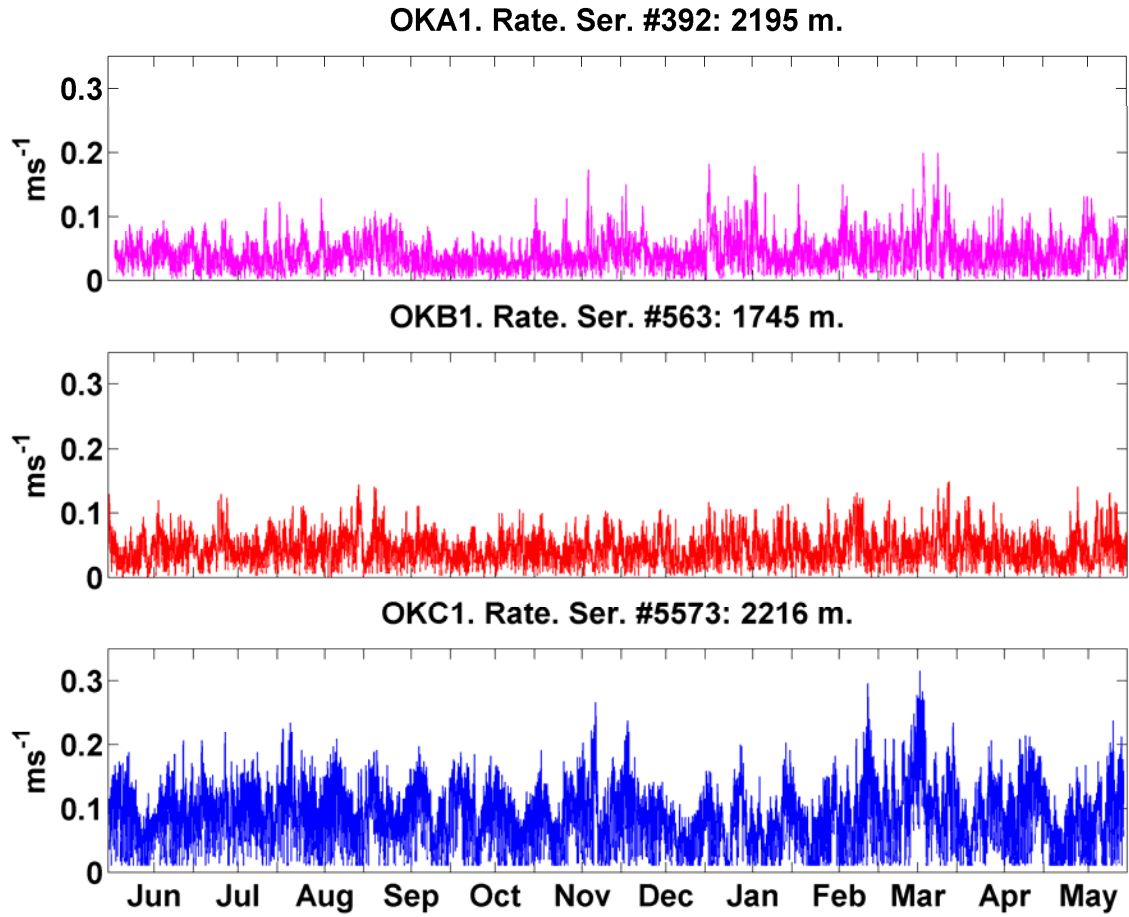


Figure 7: Current meter rate measurements at the three mooring sites on Orphan Knoll for the period May 2008 – May 2009. Locations of the moorings are provided in Figure 2.

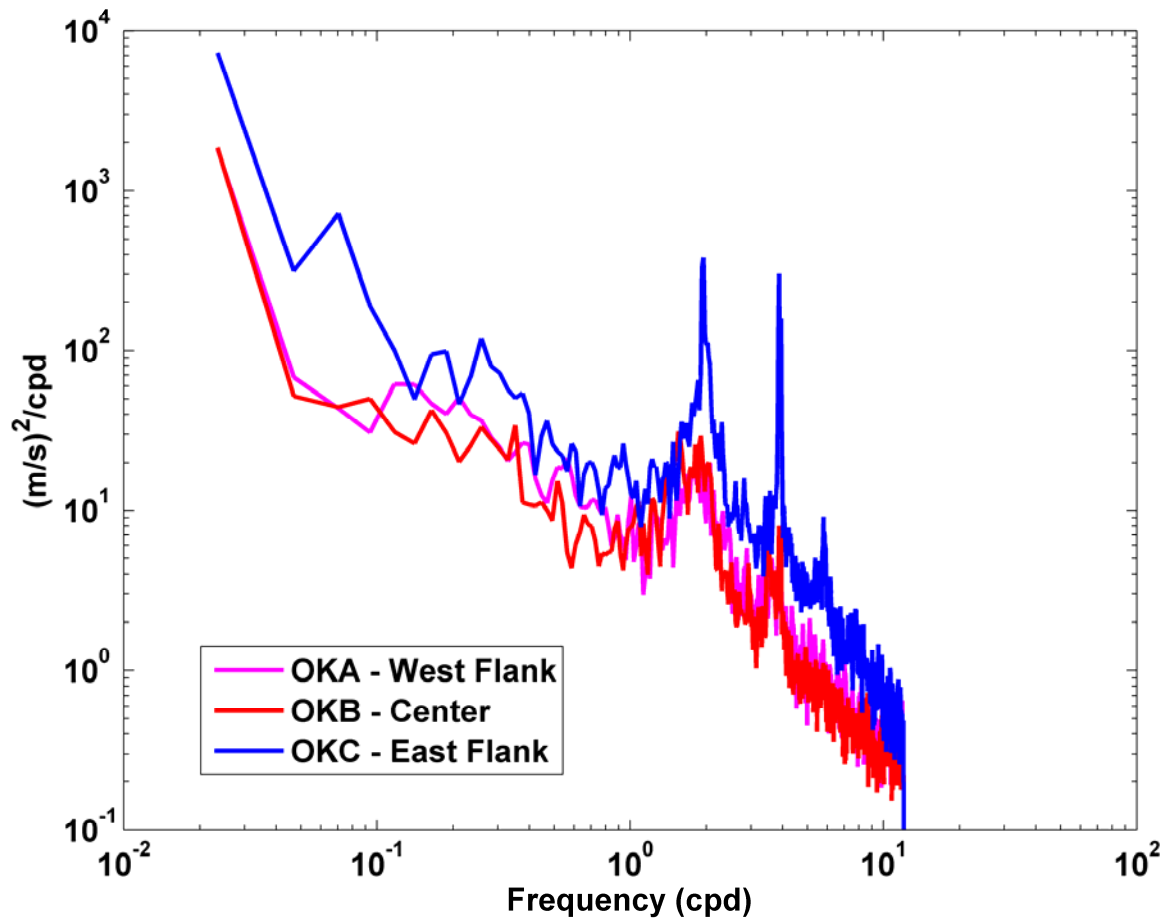
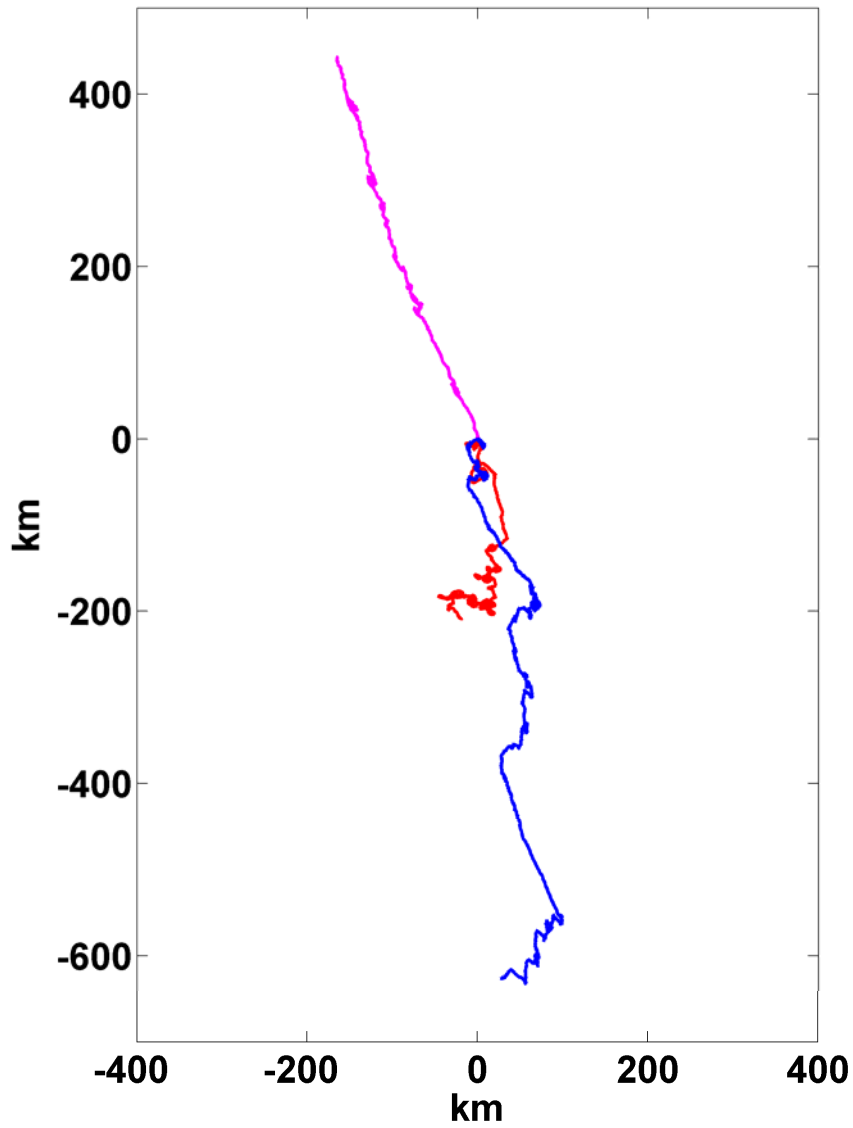


Figure 8: Power spectral density of current meter rates from time series presented in Figure 7.



**Figure 9: Progressive vector diagram demonstrating consistent flow to the northwest on the western flank of Orphan Knoll (magenta), predominantly southeast flow on the eastern flank (blue) and a reduced flow on top of the knoll relative to that measured on the flanks (red).**

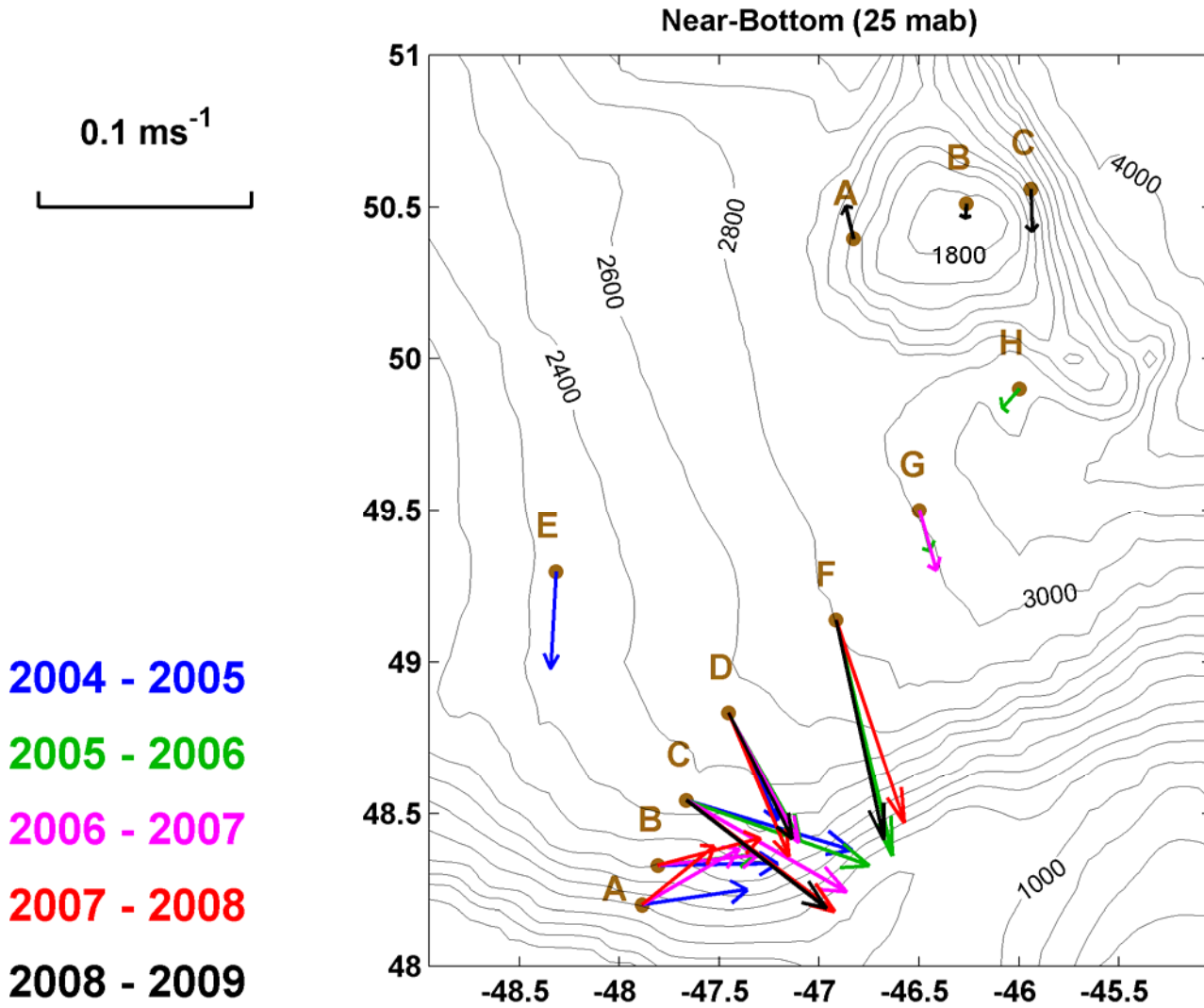


Figure 10: Mean near-bottom currents (25 metres above bottom) in the Orphan Basin and Orphan Knoll region for the years 2004-09. Color of the arrows corresponds to the legend and the scale length of 0.1 m s<sup>-1</sup> is shown.

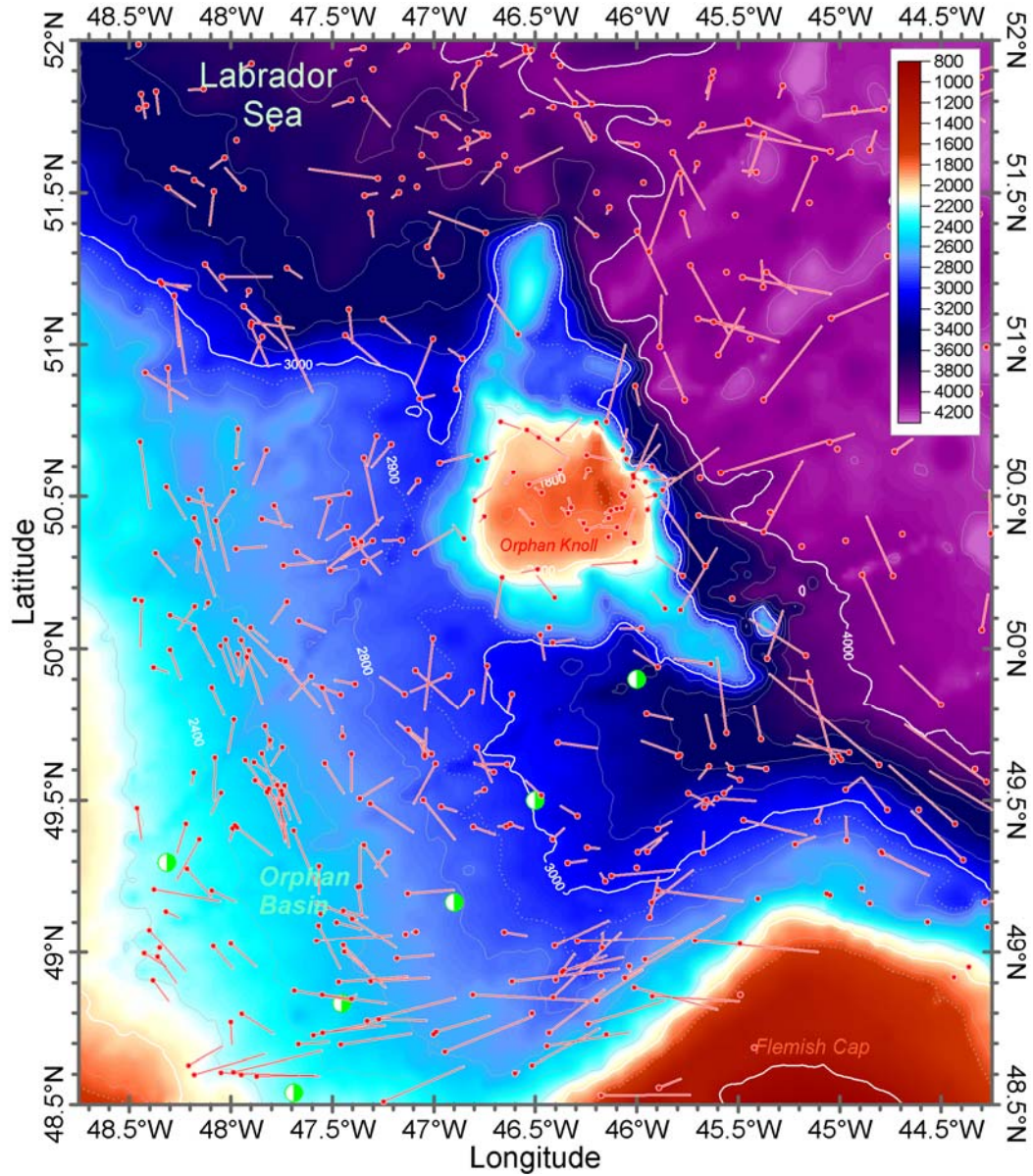


Figure 11: Argo float estimates of drift rate and direction at 1500 m depth using float position data from successive profiles.

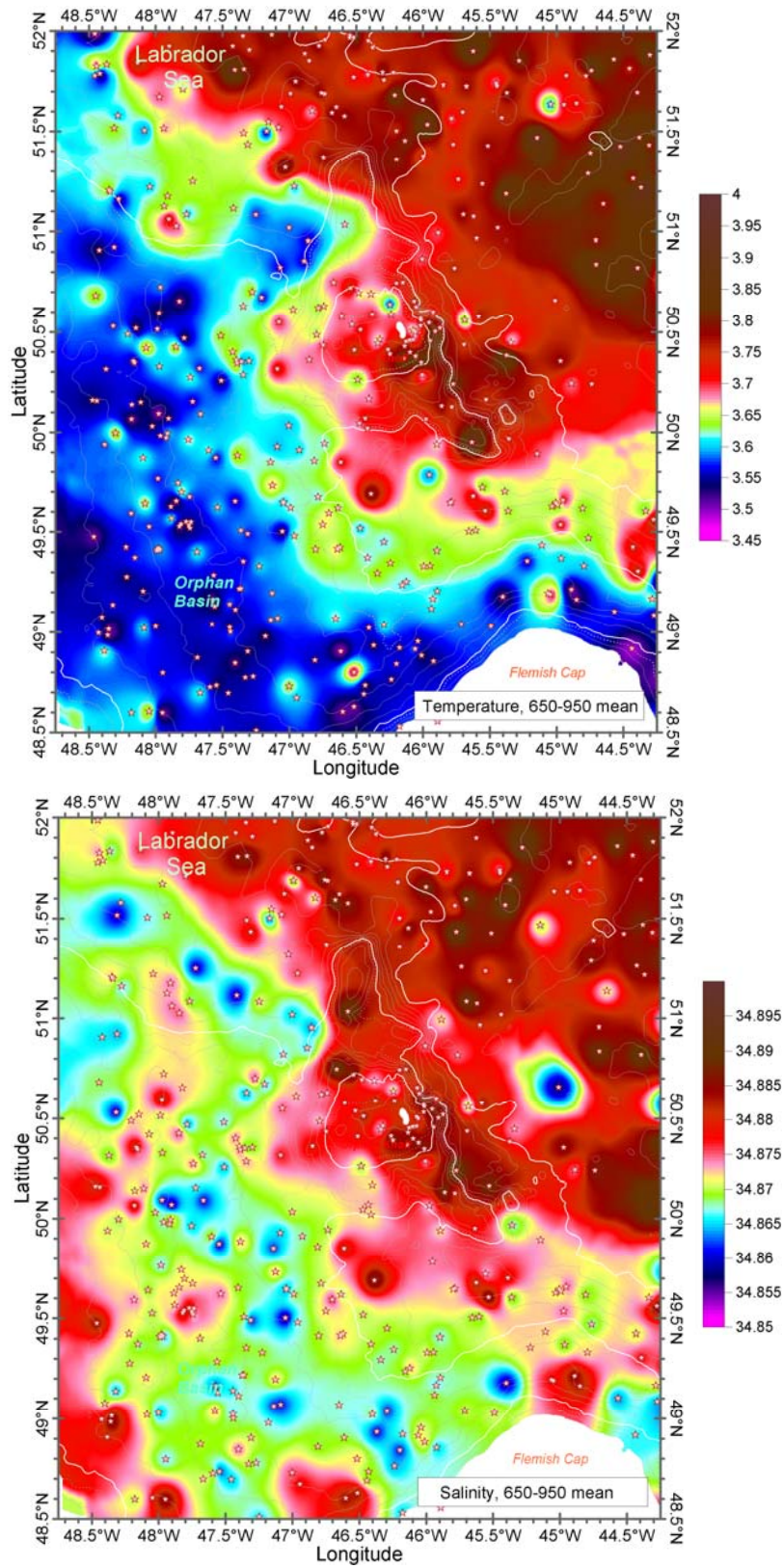


Figure 12: Temperature (top) and salinity (bottom) climatology during the period of the Argo float program for the 650-950 m layer.

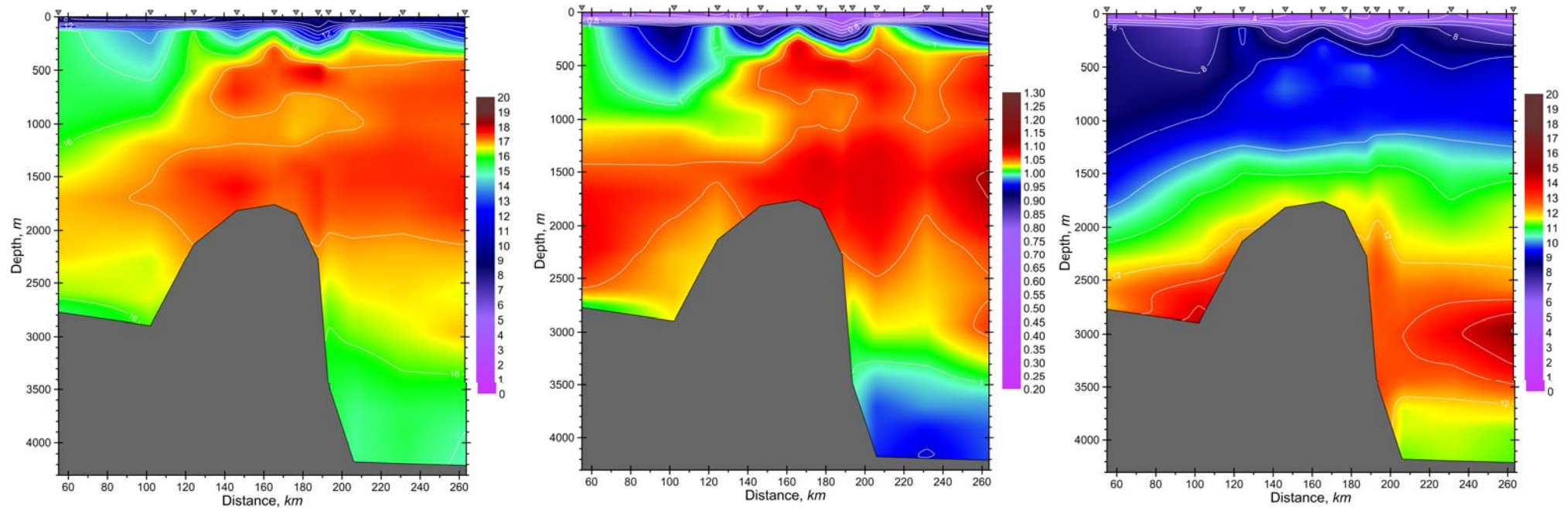


Figure 13: Nitrate (left), phosphate (center) and silicate (right) measurements from 2009 hydrographic survey of Orphan Knoll.

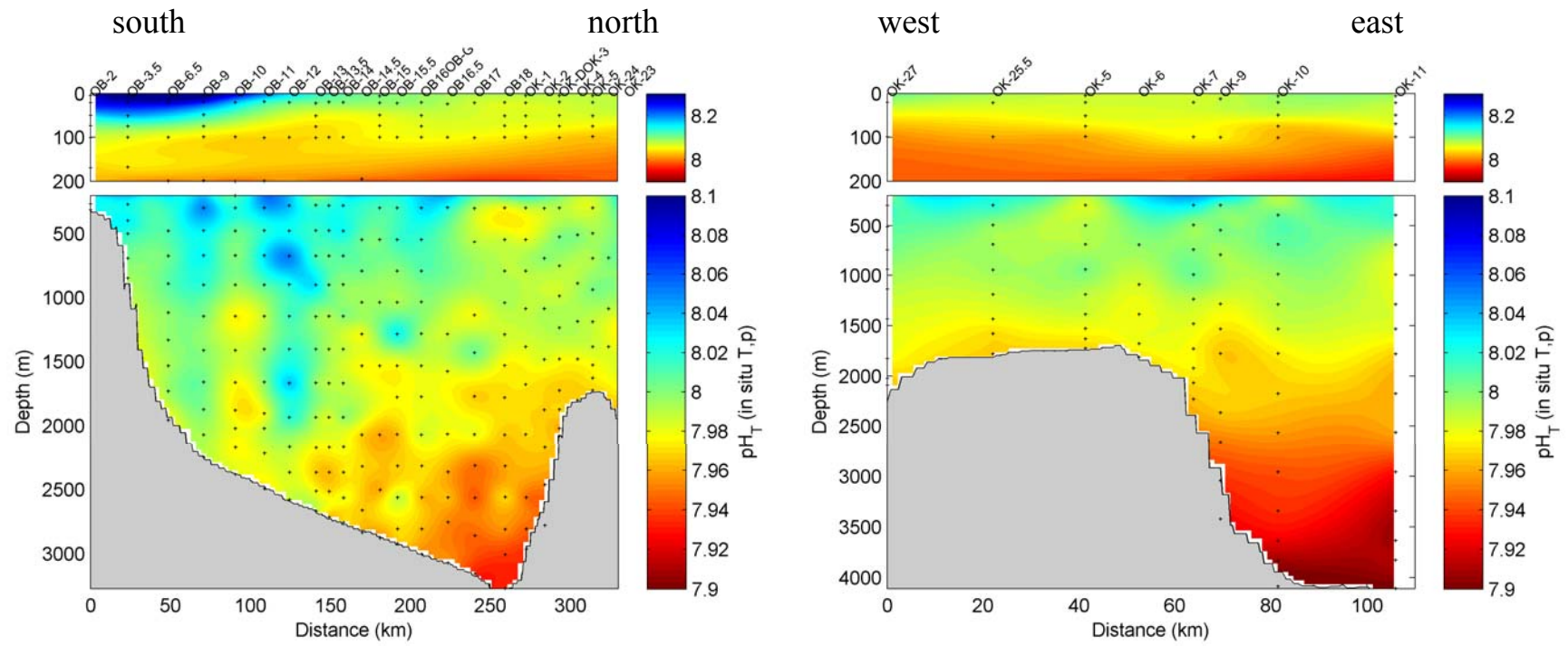


Figure 14: pH distribution along the line OBA and OBB (refer to Figure 2 for line orientation).

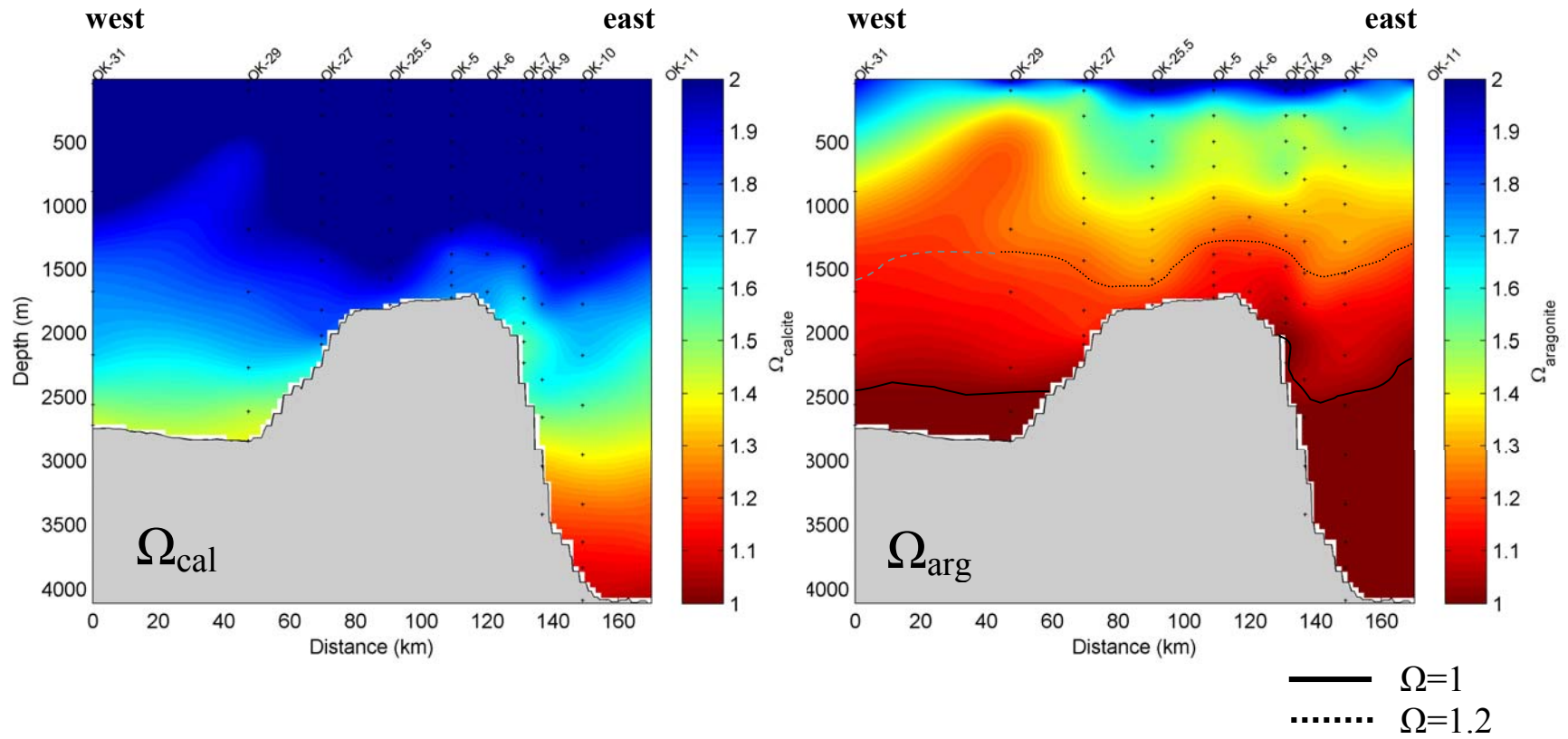


Figure 15: Saturation state of seawater with respect to calcite ( $\Omega_{\text{cal}}$ ) and aragonite ( $\Omega_{\text{arg}}$ ) along the line OBB (refer to Figure 2 for line orientation).

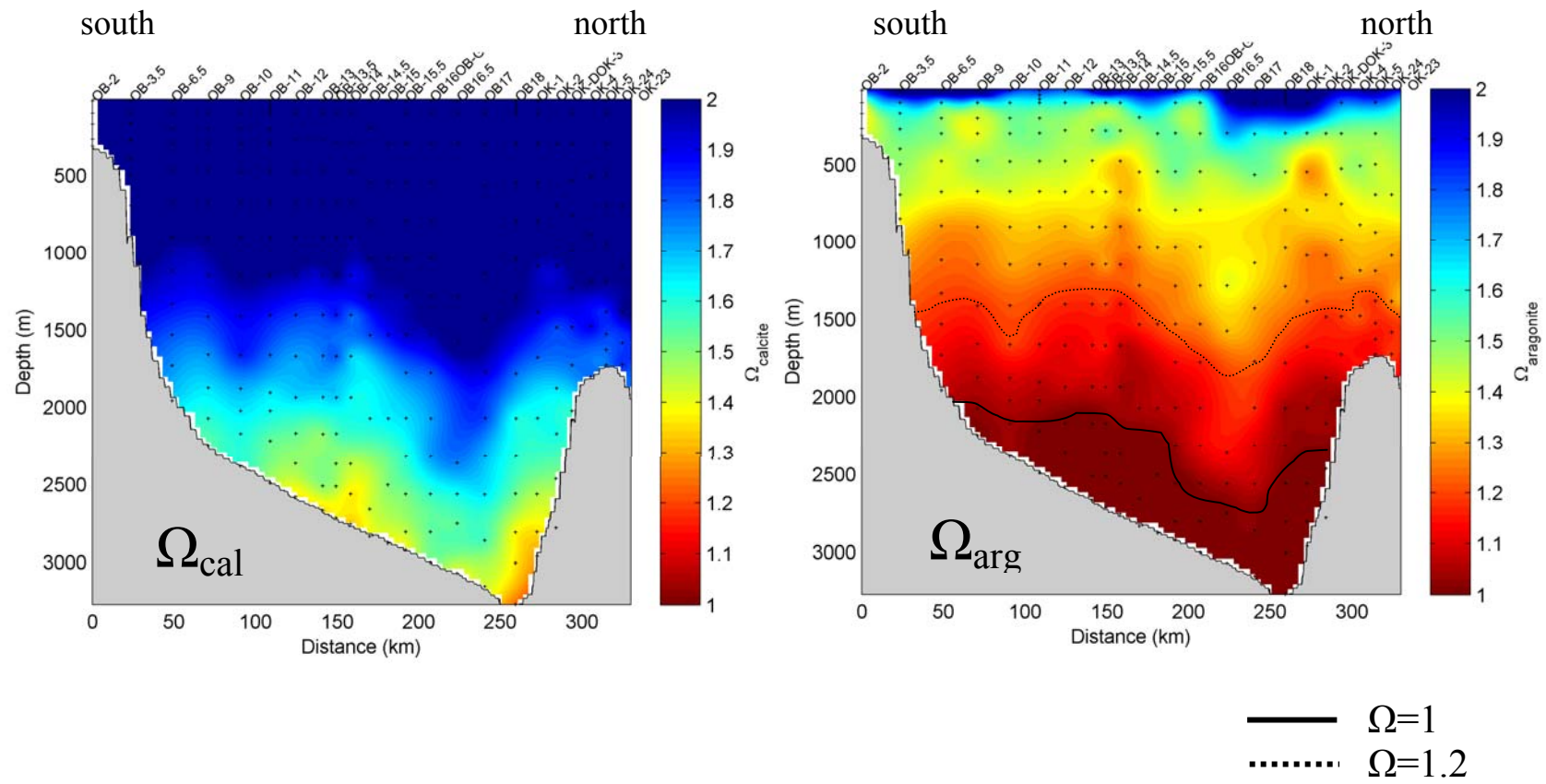


Figure 16: Saturation state of seawater with respect to calcite ( $\Omega_{\text{cal}}$ ) and aragonite ( $\Omega_{\text{arg}}$ ) along the line OBA in Orphan Basin.

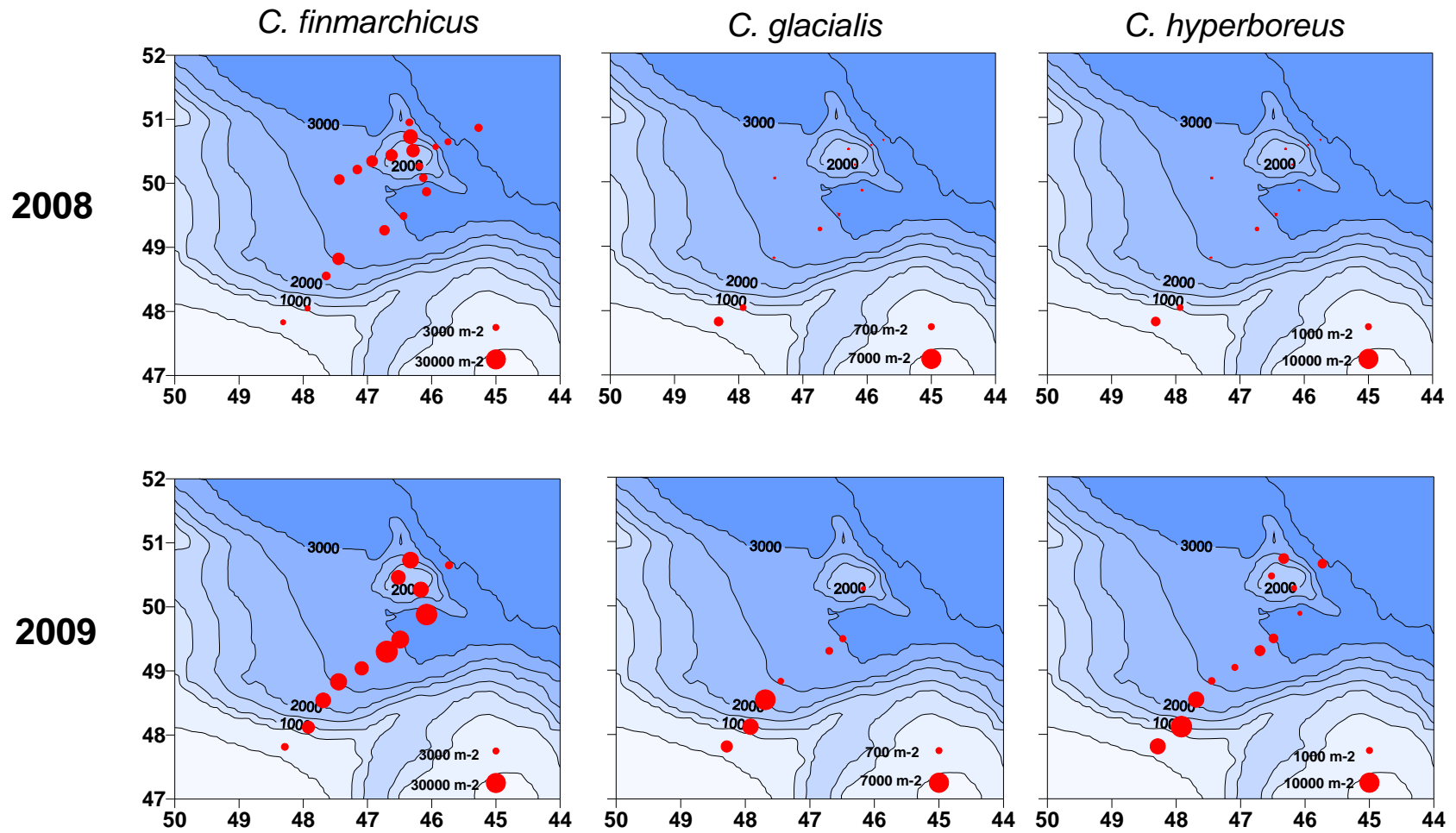


Figure 17: Distributions of three *Calanus* species (0-100 m) in the Orphan basin/Orphan Knoll region in May 2008 and 2009.

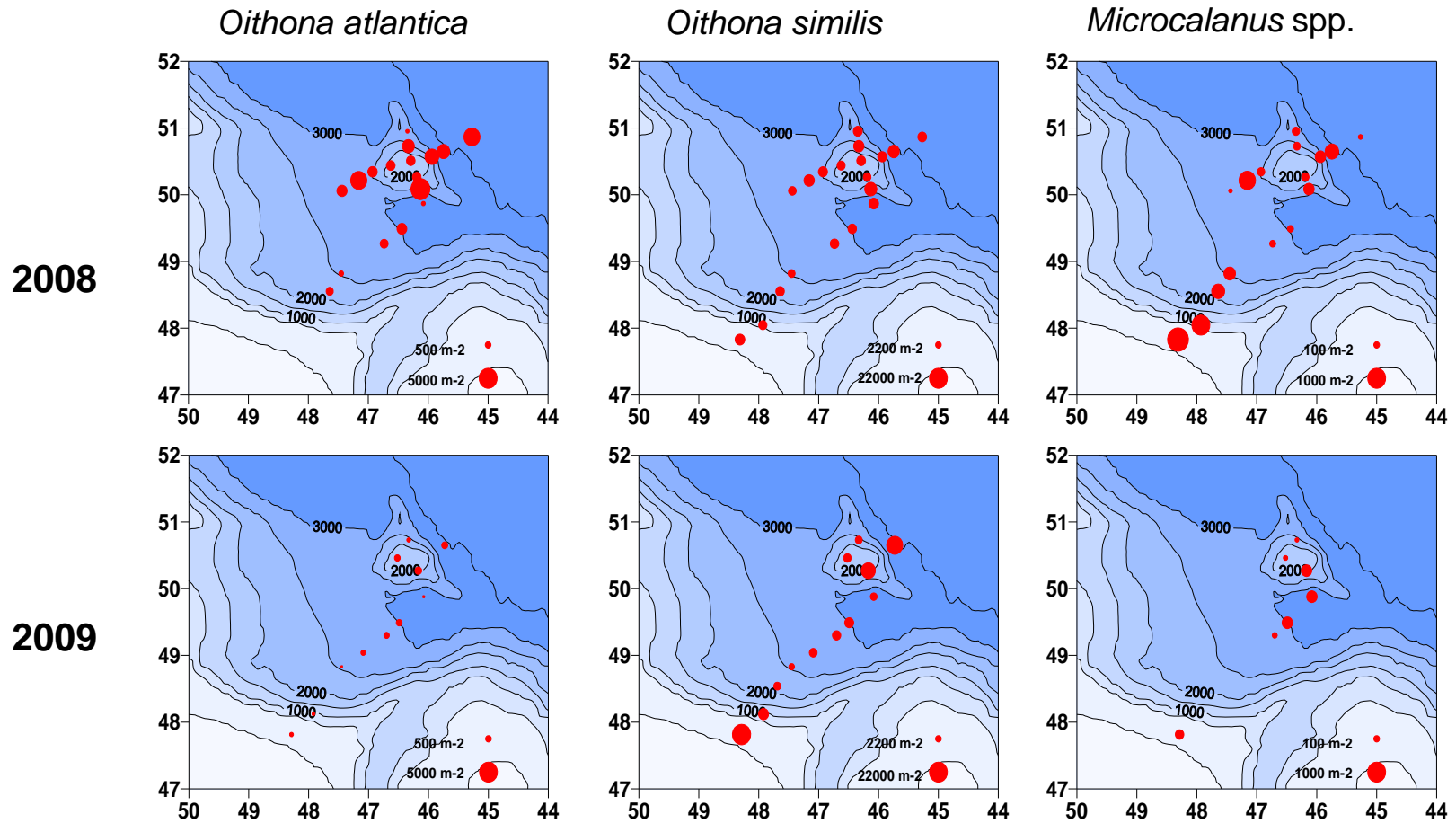


Figure 18: Distributions of *Oithona* and *Microcalanus* species (0-100 m) in the Orphan Basin/Orphan Knoll region in May 2008 and 2009.

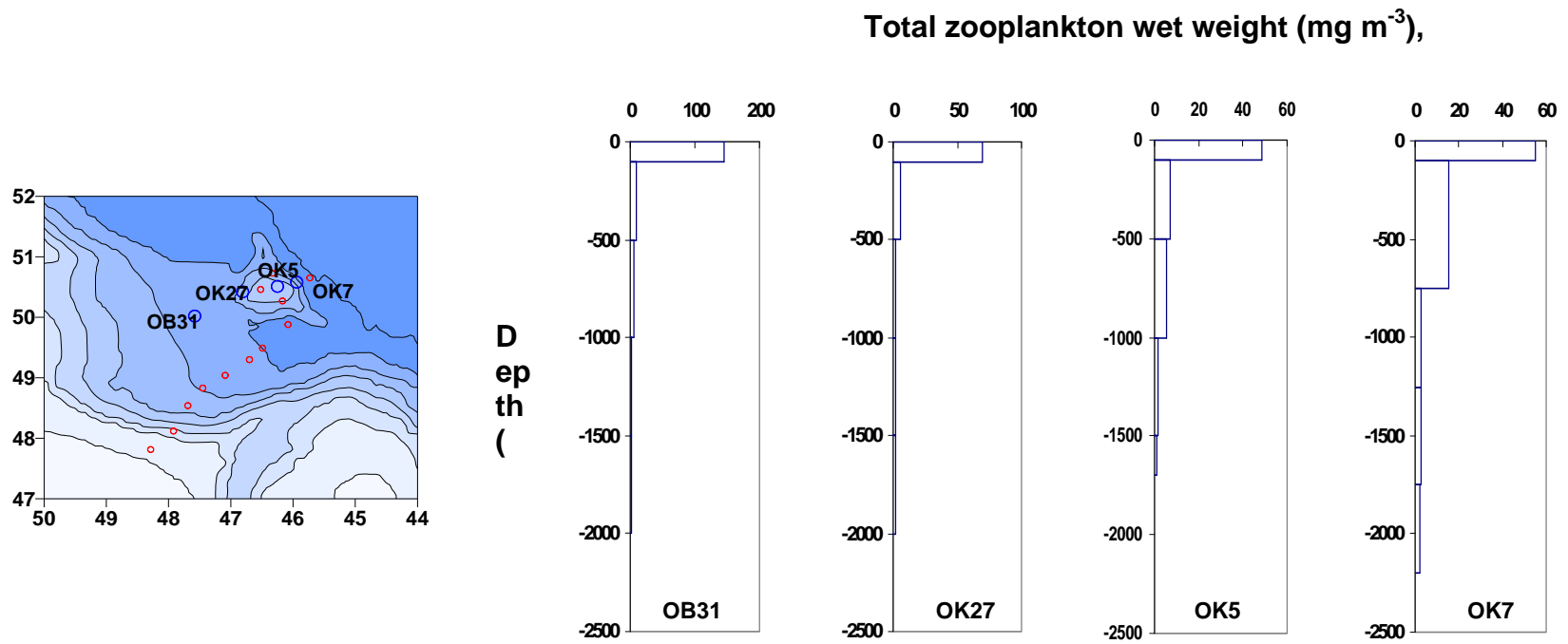


Figure 19: Positions of Multi-net stations (left) and vertical distribution of zooplankton biomass at those stations.

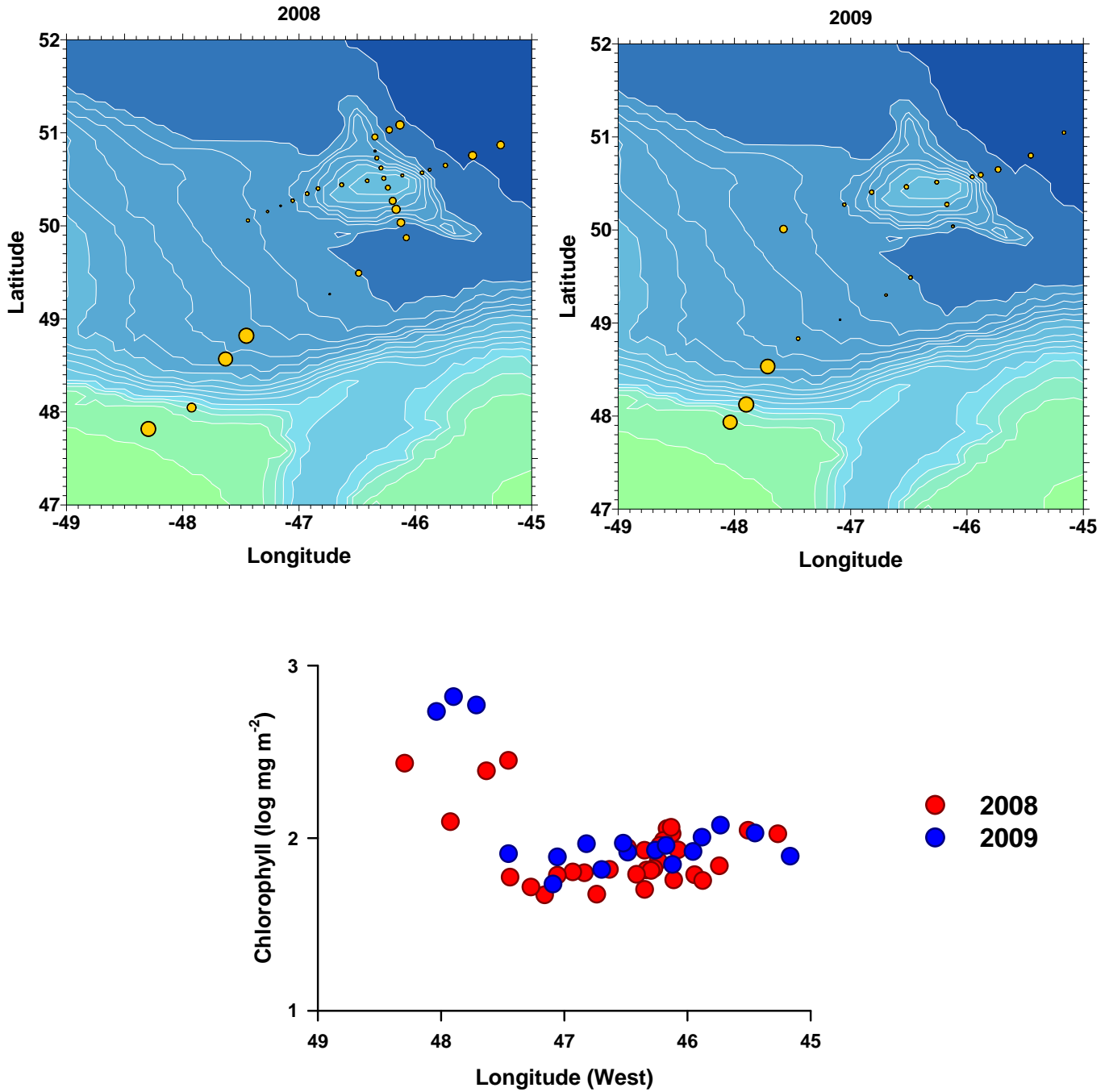


Figure 20: Vertically integrated chlorophyll concentration ( $\text{mg m}^{-2}$ ) for survey stations in Orphan Basin and Orphan Knoll. The size of the dots in the upper panels provides a relative measure of concentration.

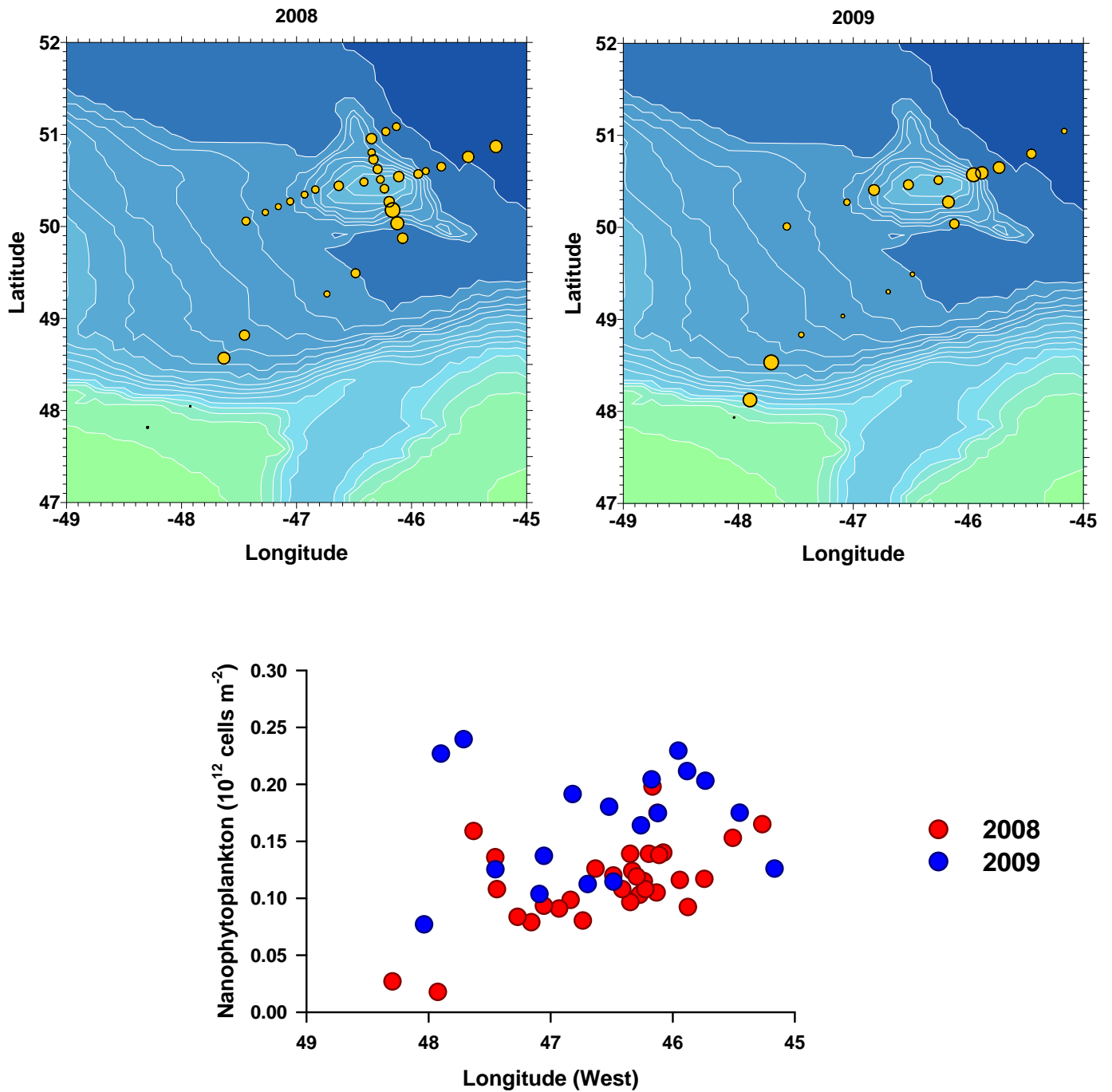


Figure 21: Vertically integrated nanophytoplankton count ( $\text{cells m}^{-2}$ ) for survey stations in Orphan Basin and Orphan Knoll. The size of the dots in the upper panels provides a relative measure of the counts.

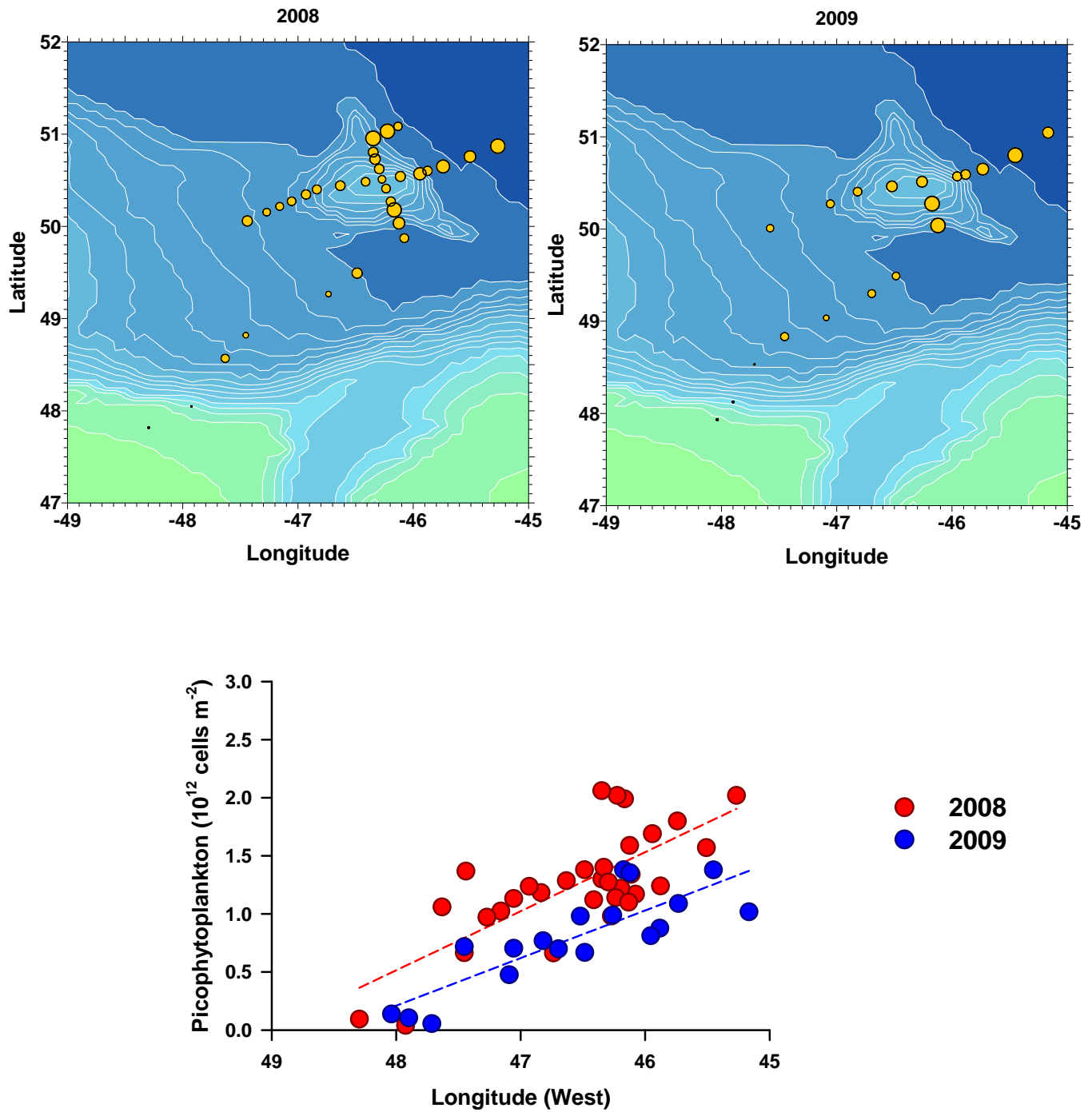


Figure 22: Vertically integrated picophytoplankton (synechococcus + picoeukaryotes ) count (cells  $m^{-2}$ ) for survey stations in Orphan Basin and Orphan Knoll. The size of the dots in the upper panels provides a relative measure of the counts.

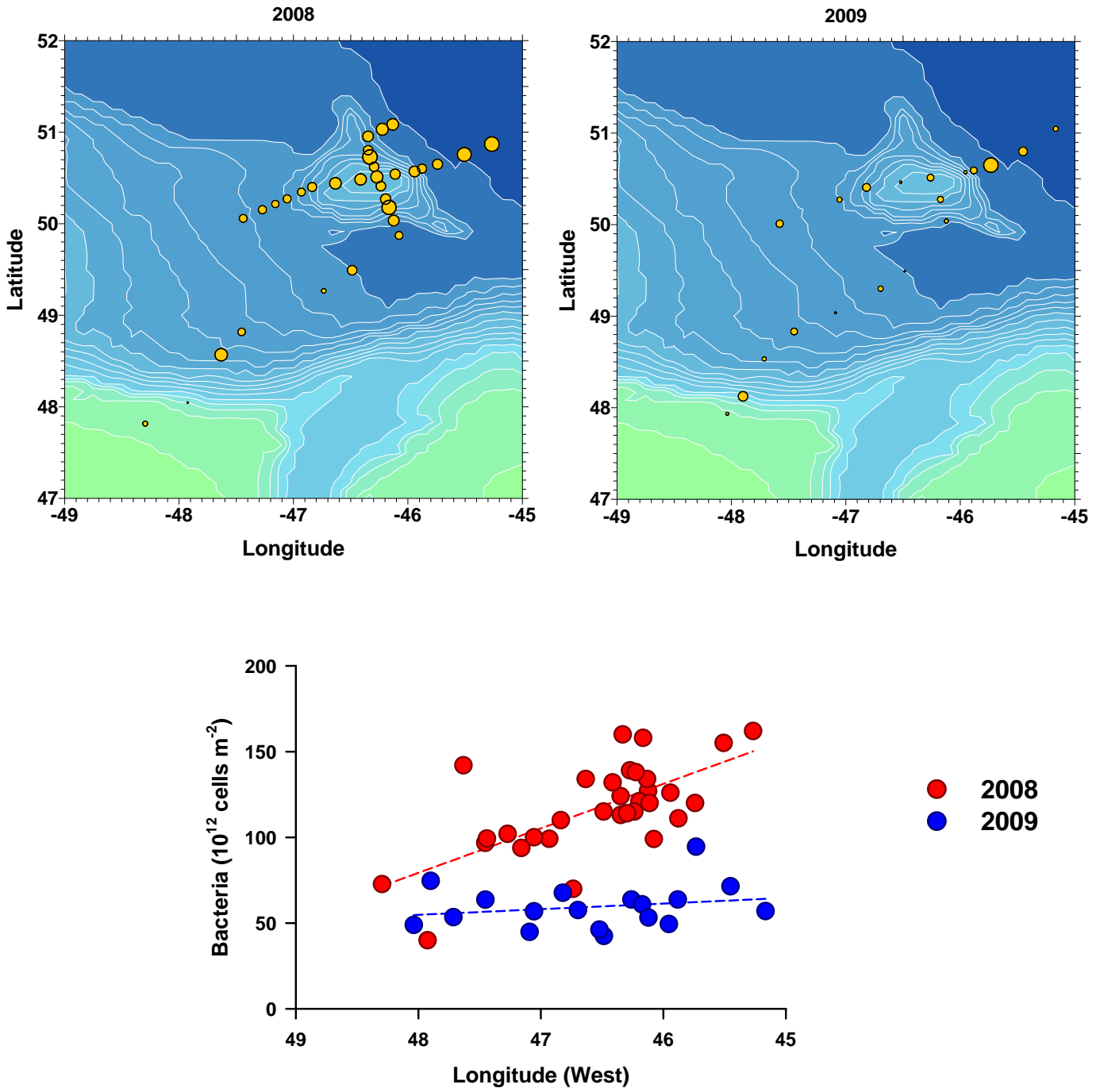
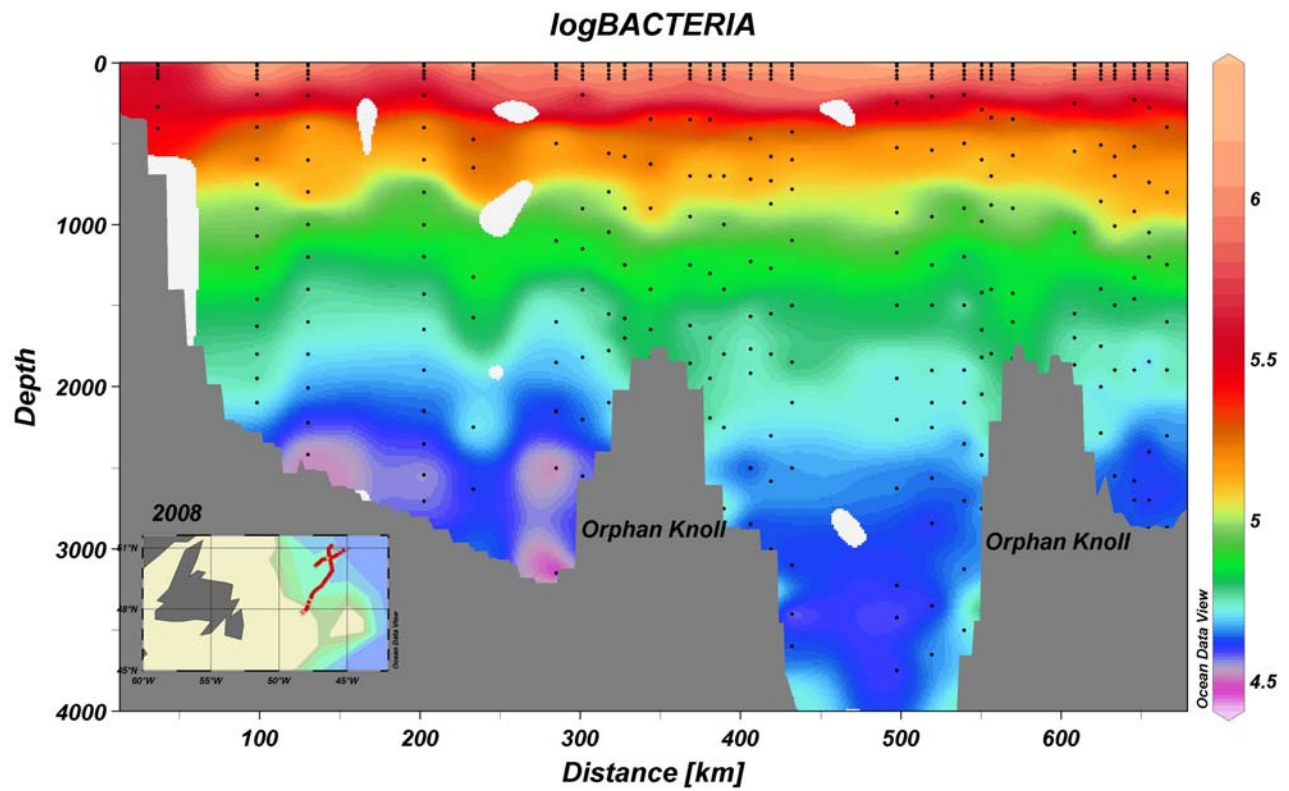


Figure 23: Vertically integrated bacteria count (cells  $m^{-2}$ ) for survey stations in Orphan Basin and Orphan Knoll. The size of the dots in the upper panels provides a relative measure of the counts.



**Figure 24: Hydrographic survey HUD2008-006 of bacterial abundance showing a local downward displacement of isopleths at depths greater than 1500m in the waters immediately overlying Orphan Knoll.**